Available online at www.sciencedirect.com

ScienceDirect

journal homepage: www.elsevier.com/locate/issn/15375110

Research Paper

Assessment of vineyard vigour and yield spatio-temporal variability based on UAV high resolution multispectral images

Massimo V. Ferro, Pietro Catania, Daniele Micciché, Antonino Pisciotta, Mariangela Vallone[*], *Santo Orlando*

University of Palermo, Department of Agricultural, Food and Forest Sciences (SAAF), Viale delle Scienze ed. 4, 90128, Palermo, Italy

ARTICLE INFO

Article history:
Received 20 November 2022
Received in revised form
17 April 2023
Accepted 1 June 2023

Keywords:
Precision viticulture
Shoot pruning weight
Vegetation index

Accurate, timely assessment of the vineyard on a field scale is essential for successful grape yield and quality. Remote sensing can be an effective and useful monitoring tool, as data from sensors on board Unmanned Aerial Vehicles (UAV) can measure vegetative and reproductive growth and thus directly or indirectly detect variability. Through the images obtained from UAV, the Vegetation Indices (VIs) can be calculated and compared with various agronomic characteristics of the vineyard. The objective of this study was to evaluate the multispectral response of the vineyard in three specific phenological phases and to analyse the spatial distribution of vegetative vigour. A multirotor UAV equipped with a camera featuring multispectral sensors was used. Four VIs namely Normalised Difference Vegetation Index (NDVI), Normalised Difference Red Edge (NDRE), Green Normalised Difference Vegetation Index (GNDVI), Modified Soil Adjusted Vegetation Index (MSAVI), were calculated using the georeferenced orthomosaic UAV images. Computer vision techniques were used to segment these orthoimages to extract only the vegetation canopy pixels. High level of agronomic variability within the vineyard was identified. Pearson's coefficient showed a significant correlation between NDVI and NDRE indices and yield since early phenological stages ($r = 0.80$ and 0.72 respectively), GNDVI at grape ripening ($r = 0.83$). Shoot pruning weight (SPW) shows the highest values of correlation ($r = 0.84$) with NDVI during the phenological stage of berries pea size. Simple linear regression techniques were evaluated using VIs as predictors of the SPW, and accurate predictive results were obtained for NDVI and NDRE with RMSE values of 0.18 and 0.24, respectively. Geostatistical analysis was applied to model the spatial variability of SPW, and thus vineyard vigour. Assessing spatial variability and appreciating the level of vigour enables improved vineyard management by increasing sustainability and production efficiency.

* *Corresponding author.*
E-mail address: mariangela.vallone@unipa.it (M. Vallone).
https://doi.org/10.1016/j.biosystemseng.2023.06.001

Nomenclature

Abbreviation	*Definition*
PV	Precision viticulture
UAV	Unmanned aerial vehicles
VI	Vegetation index
NDVI	Normalised difference vegetation index
NDRE	Normalised difference red edge
GNDVI	Green normalised difference vegetation index
MSAVI	Modified soil adjusted vegetation Index
SPW	Shoot pruning weight
RGB	Red Green Blue
TLA	Total leaf area
SLRM	Simple linear regression models
PDO	Protected designation of origin
GNSS RTK	Global navigation satellite system real-time kinematic
GPS	Global positioning system
GSD	Ground sample distance
NIR	Near-infrared
ha	Hectare
cv	Cultivar
VSP	Vertical shoot position
DOY	Day of year
VTOL	Vertical take-off and landing
CMOS	Complementary metal oxide semiconductor
MP	Mega pixel
nm	Nanometre
FOV	Field of view
a.g.l	Above ground level
TIFF	Tagged Image File Format
GCP	Ground control point
DEM	Digital elevation model
VP	Vineyard plot
SD	Standard deviation
F	Flight
HV	High vigour
MV	Medium vigour
LV	Low vigour
TSS	Total soluble solids
R^2	Coefficient of determination
r	Pearson's correlation coefficient
RMSE	Root mean square error
MAPE	Mean absolute percentage error

1. Introduction

Grapevine (*Vitis vinifera* L.) is a crop of great economic importance, widely cultivated worldwide. Vineyards' reproductive and qualitative variability is very high (Baluja et al., 2012; Barbagallo, Guidoni, & Hunter, 2011; Pisciotta, Barbagallo, Lorenzo, & Hunter, 2013), in addition to environmental factors is also influenced by anthropogenic factors regarding agronomic techniques (Pisciotta, Di Lorenzo et al., 2013). Nowadays, it's increasingly important to achieve excellent production standards, focusing on grape quality, which are influenced by several factors, such as genetic factors that distinguish cultivars and clones, or the effects of soil characteristics (Barbagallo, Vesco, Di Lorenzo, Lo Bianco, & Pisciotta, 2021), soil erosion (Novara et al., 2018), row orientation (Catania, Orlando, Roma, & Vallone, 2019; Hunter et al., 2021; Pisciotta, Catania, Orlando, & Vallone, 2019, pp. 367–374), nutrients, light, temperature and water availability (Hunter et al., 2014; Triolo, Roby, Pisciotta, Di Lorenzo, & van Leeuwen, 2019), which occur as single factors or as an interaction (Mirás-Avalos, Fandiño, Rey, Dafonte, & Cancela, 2020; Poni et al., 2018). In addition there are risks related to climatic conditions, which are expected to worsen and thus strongly impact the whole sector (Droulia & Charalampopoulos, 2021). All these factors contribute to increasing the spatial variability of vineyards, therefore information on spatial and temporal variation is essential to support farmers in decision making to enhance profitability. The estimation of the agronomic variability of each plot should be done from year to year and at different phenological stages of the vineyard (Bramley & Hamilton, 2004). Today, there are new technologies for monitoring and managing the vineyard and controlling vegetative and productive growth. Using high-resolution remote and proximal sensors, spatial variability of vine vigour can be investigated, and chemical parameters determined from grapes (Kemps, Leon, Best, De Baerdemaeker, & De Ketelaere, 2010), at any time; this information can thus be used for the variable application of many agronomic practices according to the principles of Precision Viticulture (PV) (Matese et al., 2015).

Satellite systems and Unmanned Aerial Vehicles (UAVs) that capture images in the visible and near-infrared bands of the electromagnetic spectrum are widely used to generate vegetation maps (Roma & Catania, 2022). Sensors used for crop monitoring have a specific geometric resolution, which refers to the size of the ground surface area (pixel) whose electromagnetic energy is detected. They have also a certain spectral resolution, which indicates the number of acquisition bands and their range, and a specific radiometric resolution indicating the intensity of the radiation that the sensor can identify. Finally, there is a temporal resolution which indicates the period of time between two consecutive images acquisition (Assmann, Kerby, Cunliffe, & Myers-Smith, 2018). Satellites employed for multispectral surveys are divided according to their spectral resolution (Anastasiou et al., 2018; Sun et al., 2017). These platforms can assess vineyard variability in a relatively detail in terms of resolution. On the contrary, UAVs proved to be more effective tools in representing vineyard variability as they can easily discretise the canopy from the inter-row (Khaliq et al., 2019). If satellite systems are very suitable for extensive cultivation (Sozzi et al., 2021), in other areas the use of UAVs is preferred, allowing quick surveys and providing important information for winegrowers. In general, the spectral sensors that UAVs are equipped with, have high spatial resolution and can be classified according to the method by which they achieve spectral discrimination (Sellar & Boreman, 2005). These sensors have a short ground sampling distance, and the captured images can generate high-quality dense point clouds and high-resolution orthomosaics (Aasen, Honkavaara, Lucieer, & Zarco-Tejada, 2018; Toth & Jóźków, 2016). The combination of the different bands of the electromagnetic spectrum provides important

information about the vegetative growth of crops (Pádua, Marques, Hruška, Adão, Bessa, et al., 2018). For instance, the wavelength of RGB (Red, Green, Blue) investigates the pigments present in the vegetative tissues and the status of biomass (Jannoura, Brinkmann, Uteau, Bruns, & Joergensen, 2015; Lu et al., 2021). The combination of RGB with Red Edge studies the efficiency of chlorophyll pigments, whereas the prediction of biophysical parameters is carried out by investigating the Red and Near-Infrared spectrum regions (Giovos, Tassopoulos, Kalivas, Lougkos, & Priovolou, 2021). Vegetation mapping is performed by calculating different Vegetation Indices (VIs) from specific wavelengths (Xue & Su, 2017) and is often used to estimate plant growth parameters.

An equally important issue is the relationship between multispectral indices and vegetative vigour; it's known that there is a close relationship between Normalised Difference Vegetation Index (NDVI) and vigour (Costa Ferreira et al., 2007, pp. 1372–1381). A distance-based index commonly used in PV is Modified Soil-Adjusted Vegetation Index (MSAVI); it reduces the soil disturbance effect and produces more accurate vineyard vegetation assessment (Tassopoulos, Kalivas, Giovos, Lougkos, & Priovolou, 2021). The Normalised Red Edge Difference Index (NDRE) and the Green Normalised Difference Vegetation Index (GNDVI), are able to provide information on the health status of grapevine's through determining the variability of vegetation physiological parameters (Daglio et al., 2022; Tosin, Martins, Pôças, & Cunha, 2022). The agronomic estimation of vine vigour is often carried out by assessing the Shoot Pruning Weight (SPW) (Rey-Caramés, Tardaguila, Sanz-Garcia, Chica-Olmo, & Diago, 2016). SPW is related to the vegetative biomass in the growing season and, therefore, to vine vigour. Among the vegetative growth parameters it is distinguished by its high sensitivity to variations in soil fertility and water availability (White, 2015). SPW is used to assess the relationship between vegetative and reproductive growth by calculating the Ravaz index (Taylor & Bates, 2012), which is an indicator of vine balance and grape quality (Smart & Robinson, 1991). The predictive study of SPW is a topic that has always attracted much interest; knowing in advance how the variability of this vigour parameter is distributed, allows to manage vines by balancing vegetative-productive development. It is reported in the literature that pruning weight correlates well with multispectral indices or RGB imagery (Caruso et al., 2017; Dobrowski, Ustin, & Wolpert, 2003; García-Fernández, Sanz-Ablanedo, Pereira-Obaya, & Rodríguez-Pérez, 2021; Rey-Caramés, Diago, Martín, Lobo, & Tardaguila, 2015). Positive spatial autocorrelations were found through comparisons made between SPW and NDVI data of the vineyard canopy surveyed by UAV (Pastonchi, Di Gennaro, Toscano, & Matese, 2020). Many authors separate SPW values into different vigour classes and identify equally differences in NDVI class data, using different monitoring platforms (Bonilla, Toda, & Martínez-Casasnovas, 2013; Caruso et al., 2017; Filippetti et al., 2013; Gatti, Garavani, Vercesi, & Poni, 2017). Matese and Di Gennaro (2018) demonstrated that using UAVs allows for obtaining both detailed spectral information that correlates well with SPW and also optimal correlations with canopy geometric characters, such as thickness (Matese & Di Gennaro, 2021).

Leaf Area Index (LAI) is another relevant index applied for assessing vigour spatial variability. The estimation of this canopy parameter using multispectral and hyperspectral images taken by UAV has given positive results (Kalisperakis, Stentoumis, Grammatikopoulos, & Karantzalos, 2015; Siegfried, Viret, Huber, & Wohlhauser, 2007).

The estimation of yield parameters using UAV-derived data is demonstrated to be very efficient; in fact, an assessment of spatial variability indicates common behaviour in high vigour zones where higher yields and higher total acidity values are associated. In turn, low vigour zones exhibit higher pH and higher soluble solids. In opposition, medium vigour zones are associated with greater leaf area, high values of shoot pruning weights and average bunch weights (Ferrer et al., 2020; Gatti et al., 2017). In López-García et al. (2022) RGB imagery provides better yield prediction results at the beginning of the grapevine growing season, in contrast with multispectral data at the phenological stages of fruit set and at ripening. The estimates of yield at the beginning of the growing season allow farmers to perform cultural practices to adjust yield, reducing production quantity but increasing quality. The identification of vineyard areas with different productive and qualitative potentials makes it possible to apply selective harvesting by selecting grapes with different compositions and processing them according to their properties (Bramley, 2022; Gatti et al., 2019). Using Variable Rate Technology (VRT), the effects of uneven plot vigour could be reduced, for instance by setting up fertilisation based on the real needs of the vines (Sozzi et al., 2020, pp. 343–347). Plant protection dosage based on spatial variability uses Variable Rate Application (VRA) and is adapted to the vines' requirements. By exploiting these innovations, significant pesticide savings can be achieved without compromising treatment efficacy (Campos et al., 2020; I. del-Moral-Martínez, Rosell-Polo, Uribeetxebarria, & Arnó, 2020; Gil et al., 2013; Román et al., 2020).

Although spectral reflectance indices have been extensively used to evaluate the characteristics of various crops, the information on the performance of some indices, which differ from the commonly used NDVI, is not very thorough. Furthermore, the evaluation of these indices at different phenological stages can improve knowledge on the prediction of a given agronomic variable.

This study aims at determining vineyard spatio-temporal variability based in UAV high resolution multispectral images, in order to optimise the vineyard management. In particular, vineyard multispectral orthoimages were used to detect some agronomic parameters, to assess the vegetative growth and to determine grape yield variability. Four vegetation indices and their relationship to vegetative growth and yield were examined, providing more detailed information to winegrowers for the management of crop operations. The spatial variability of SPW was also determined by assessing the most correlated multitemporal VI of the vineyard canopy.

2. Materials and methods

2.1. *Experimental site*

The study was carried out during the 2021 growing season in a 15 years old vineyard, cultivar Catarratto, grafted onto

rootstock 1103 Paulsen. The experimental site was located within the Alcamo Protected Designation of Origin (PDO) area, in the hinterland of western Sicily (Italy) at Tenuta Rapitalà farm (37°55′9.61″N; 13° 4′28.59″E).

The vineyard is located at an altitude of 315 m above sea level and is drip irrigated (600 m^3 ha^{-1}). The plot has an extension of 8.2 ha and a perimeter of 1162 m, with layout of planting 2.40 × 1.00 m (4170 plants ha^{-1}). The rows orientation is NE–SW (Fig. 1), with an angle to the North of about 22°. The terrain is slightly hilly, with slopes of approximately 12% on the steepest line.

Vines were vertically trained (VSP trellis system) and double cordon spur pruned with two buds per spur, spaced at approximately 0.20 m. Catarratto is an ancient white variety of the Italian grapevine assortment. It is a vigorous, medium-late-ripening grapevine cultivar, widely cultivated in western Sicily. The vineyard has been managed following ordinary agronomic practices conducted uniformly on the whole field. The vineyard was traditionally managed with five passes of superficial tillage (0.1 m depth) during the year to control weeds and water evaporation and to prevent soil cracking. A mineral soil fertilisation was carried out at DOY82. Pest management practices to produce healthy grapes were applied. Figure 2 shows the meteorological data in the examined area during the period under consideration. The 2021 season was hot and dry, a typical hot arid climate.

Taking the period from 1 April to the end of October, the amount of average daily temperatures that directly influence the vine growth and grape ripening season, the Winkler index, can be computed. In this case, it was 2300 °C, a value often observed in Mediterranean areas and exacerbated by heatwaves, while the total rainfall during the 2021 season was 810 mm.

2.2. *Aerial platform and multispectral sensors used*

The remote images were acquired with a UAV, a Da-Jiang Innovations (DJI) quadcopter model Phantom 4 (DJI, Shenzhen, China), classified as VTOL (Vertical Take-Off and Landing). The UAV can carry a maximum payload of 477 g for 20–30 min with a maximum flight range of 7 km. The flight autonomy of the UAV is approximately 30 min, guaranteed by a LiPo 4S battery with a capacity of 5870 mAh and a voltage of 15.2V. Three batteries were used to survey the entire plot. The Phantom 4 was used to acquire RGB and multispectral images; it was equipped with a camera composed of six 1/2.9" CMOS sensors, mounted on the UAV using a two-axis carbon fibre gimbal, one RGB sensor for visible light images, and five monochrome sensors for multispectral image acquisition. The gimbal mitigated airframe vibration (pitch and roll) caused by wind and allowed pointing vertically downwards for image collection. Multispectral sensors operate in the bands of blue (B): 450 nm, green (G): 560 nm, red (R): 650 nm, red-edge (RE): 730 nm, and near-infrared (NIR): 840 nm, with a resolution of 2.08 MP. Each sensor has a spectral sensitivity range of ±16 nm respect to its nominal wavelength, except the NIR sensor which has a spectral sensitivity range of ±26 nm (Tominaga, Nishi, & Ohtera, 2021). The features of the camera are focal length 5.74 mm, image size 1600 × 1300 pixels, angle of view (FOV) 62.7° and aperture f/2.2. Radiometric calibration is performed based on the irradiance measured in real-time by the sensor located on the top of the UAV. In addition, a radiometric calibration was applied to the image blocks, using reference images from a

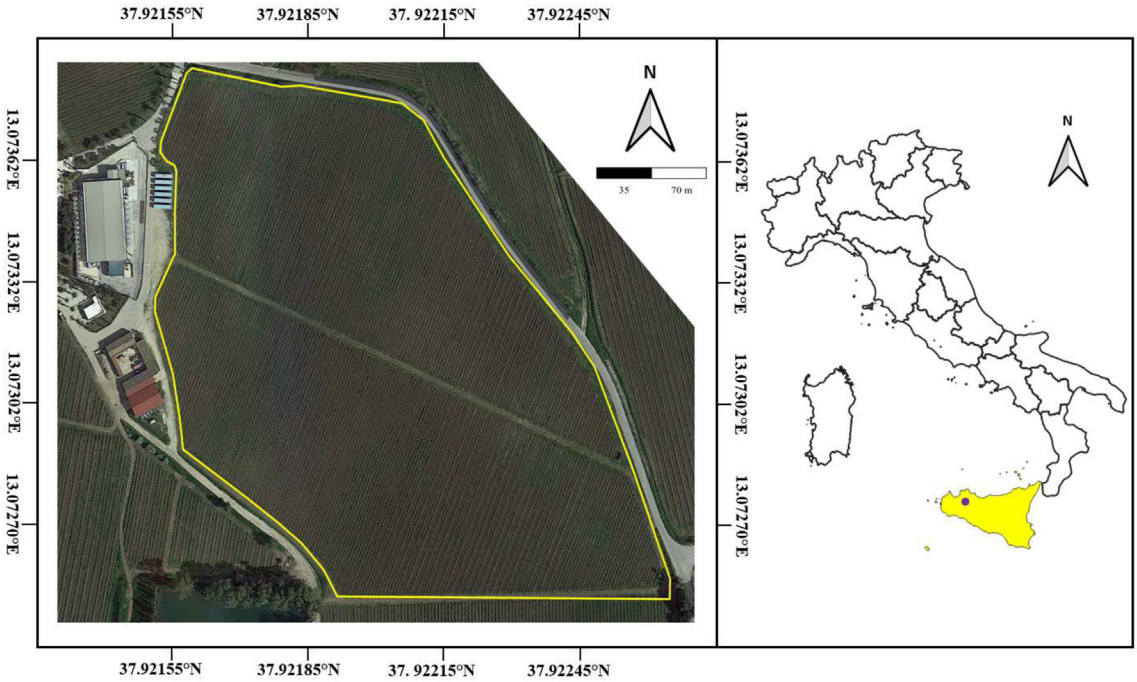

Fig. 1 – Location of the experimental vineyard in Sicily, south Italy (WGS84).

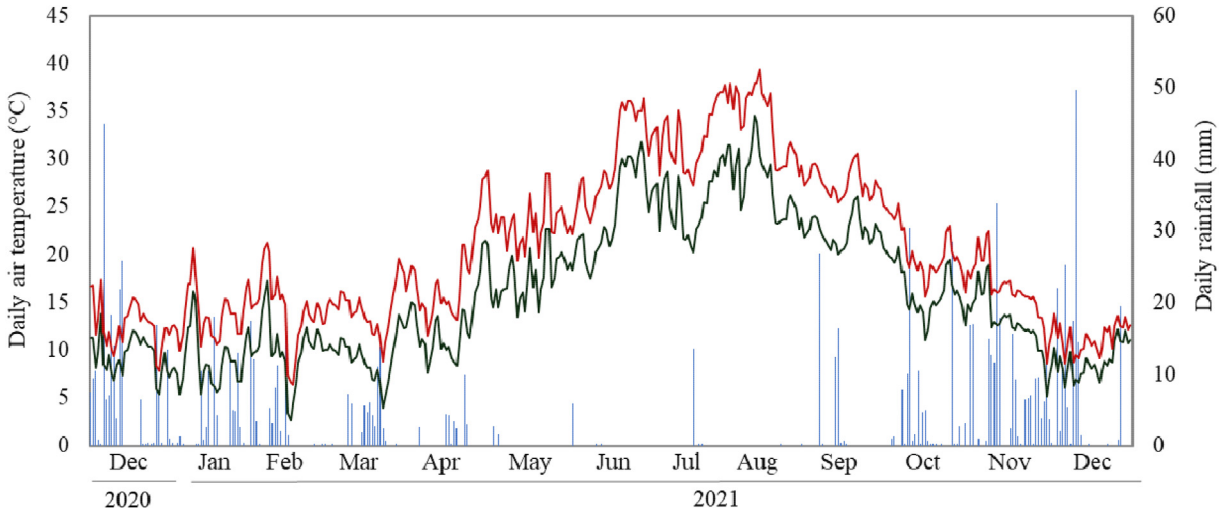

Fig. 2 – Daily maximum (–) and mean (–) air temperature and daily rainfall (–) were recorded from the beginning of November 2020 to the end of December 2021, nearby the experimental vineyard. (Sicilian Agrometeorological Information System; SIAS).

calibrated reflectance panel (LABSPHERE INC., North Sutton, US).

2.3. *Data acquisition*

The flight sessions performed with the UAV were conducted with 70% forward overlap and 70% lateral overlap at ≈70 m a.g.l height from the take-off point in a dual-grid configuration, obtaining an image pixel size (GSD) of approximately 3.7 cm for RGB and multispectral images (Fig. 3). The field of view (FOV) was 51.50 × 41.25 m and the flight speed was 20 km h^{-1}. The camera takes photos automatically, at an interval of 1 s, and the image is stored in TIFF format.

Three flight sessions were carried out during the 2021 vegetative season in different vine phenological stages (scale Biologische Bundesanstalt, Bundessortenamt und CHemische Industrie, BBCH, according to Lorenz et al., 1995) (Table 1). The first flight was performed at berries pea size (BBCH 75), while the second at beginning of ripening (BBCH 81). The last flight was made close to ripening, at full ripening (BBCH 89). Surveys were conducted during these phenological stages based on the physiological vine behaviour corresponding to the ripening process. The flight operations were scheduled from 11:30 AM to 01:00 PM.

The weather data summarised in Table 1 relate to the three flight dates, giving information about brightness, measured by irradiance, and wind conditions, both in terms of speed and direction, referred to the hours of the day when the flights took place. During the flights, there was excellent light, the wind speed was very low, and the conditions were optimal for carrying out the surveys.

2.4. *Data processing*

The georeferenced multispectral images were mosaicked using Agisoft Metashape Professional Edition (Agisoft LLC St. Petersburg, Russia - https://www.agisoft.com/). A high-resolution orthophoto 3.7 cm $pixel^{-1}$) in GeoTIFF format and a Digital Elevation Model (DEM) of the experimental vineyard were created. The first post-processing operation was to align the orthoimages. Automated procedures (batch processing) were then carried out to generate the dense points cloud and the generation of the multi-band orthomosaic. To assure the accuracy of the image, the ground control point (GCP) method was applied for geometric correction, fixing 14 points using a GPS receiver on the entire plot (Catania et al., 2020).

Using the software QGIS version 3.22. It was possible to calculate some vegetation indices (Table 2); indeed, based on the generated orthomosaic, the NDVI was calculated using the NIR bands at a wavelength of 840 nm and the red band at a wavelength of 650 nm (Rouse Jr et al., 1974). The GNDVI, that is directly proportional to leaf chlorophyll concentration at wavelengths of 540 nm and 760 nm was also used (Candiago, Remondino, De Giglio, Dubbini, & Gattelli, 2015; Gitelson & Merzlyak, 1998; Maccioni, Agati, & Mazzinghi, 2001). The NDRE was also evaluated, providing useful information on the ecophysiological state of the crop (Barnes et al., 2000). Previous research observed a sudden change between the Red and NIR reflectance of vegetation in what is known as the Red Edge band. This zone marks the boundary between chlorophyll absorption in the red band and scattering due to the internal structure of leaves in the NIR band (Jorge, Vallbé, & Soler, 2019). The MSAVI was also considered; this is the soil-adjusted vegetation index that attempts to address some of the limitations of NDVI when applied to areas with a high degree of the exposed soil surface, at wavelengths of 640 nm and 760 nm (Candiago et al., 2015; Martínez & Gomez-Miguel, 2017; Qi, Chehbouni, Huete, Kerr, & Sorooshian, 1994).

After computing the vegetation index maps, it was necessary to identify and segment the vineyard canopy from the soil and weeds by applying the unsupervised k-means segmentation algorithm as applied by (Cinat, Di Gennaro, Berton, & Matese, 2019). The principle is to segregate k groups of similar pixels (clusters) from other groups of dissimilar pixels within the raster (Fig. 4). The k-means segregates clusters based on their mean value (Galambošová, Rataj, Prokeinová, &

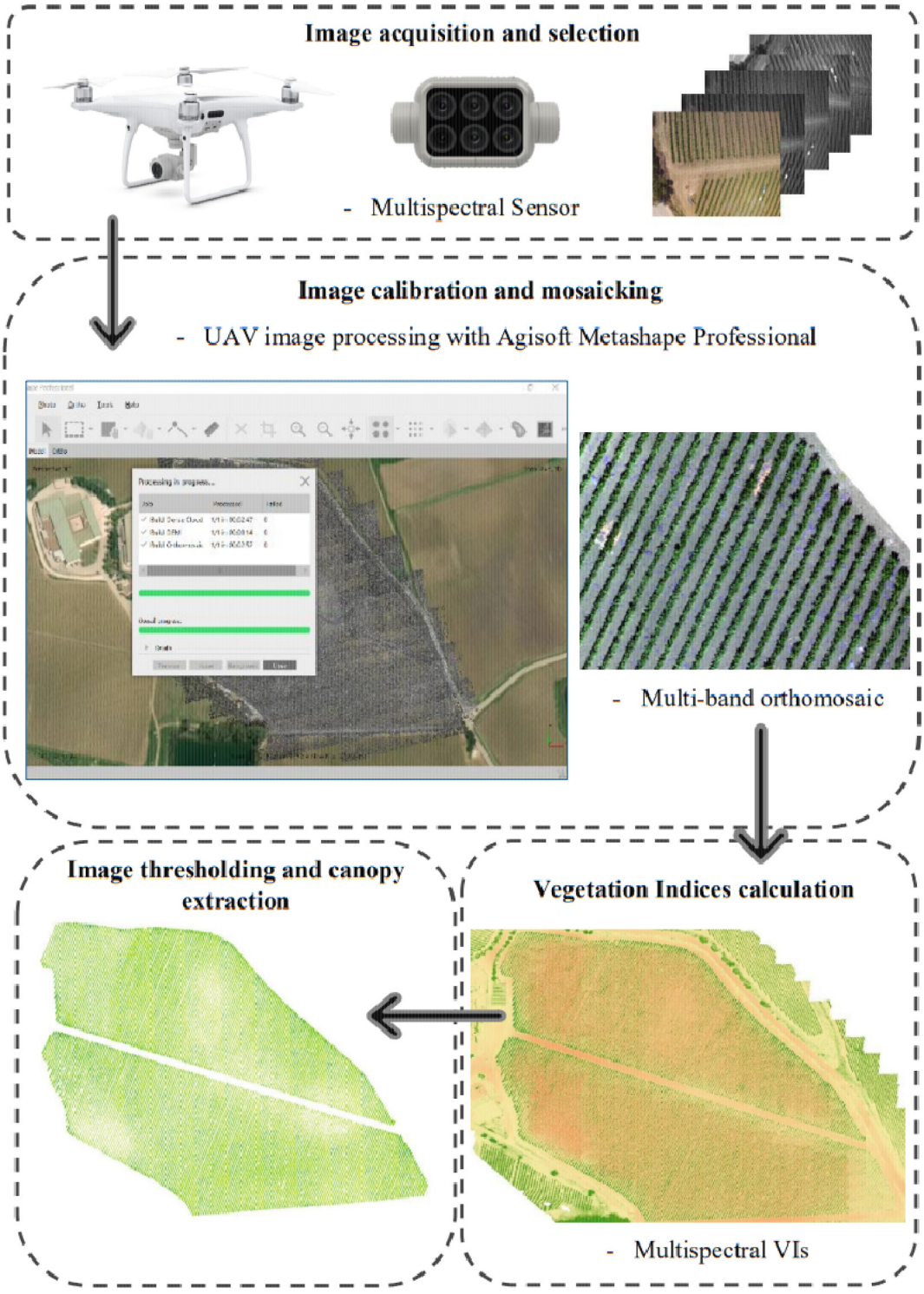

Fig. 3 – Procedure for vegetation indices calculation using multispectral images acquired by UAV.

Prešinská, 2014; Javadi, Guerrero, & Mouazen, 2022). The algorithm produced a 1-bit image, with pixels assuming values equal to zero for the soil and 1 for the vegetation as Digital Number (DN). The mask thus obtained was multiplied by the NDVI map using the QGIS raster calculator, in order to assign zero to all the soil pixels (0 = NULL) and leave the DN of the vegetation pixels unchanged. Through a new k-means classification (k = 3), the latter made it possible to identify the management areas with low (LV), medium (MV) and high (HV) vigour.

2.5. *Plant sampling and measurements*

At full ripening (BBCH 89), fourteen vineyard blocks belonging to different areas of the vineyard, showing diverse vigour, were identified, forming the Vineyard Plot 1 (VP1). Each block

Table 1 – Remote sensing data acquisition during the 2021 growing season. Meteorological data logged by the station closest to the surveyed area (Sicilian Agrometeorological Information System; SIAS).

UAV flight missions					
Acquisition time	Growth stage	DOY	Radiation (MJ/m^2)	Wind Speed (m/s)	Wind direction
18 June 2021	BBCH 75	169	26.40	1.62	N–O
21 July 2021	BBCH 81	202	27.80	1.57	S–E
28 August 2021	BBCH 89	239	25.84	1.68	S–O

Table 2 – Vegetation indices and equations used.

Vegetation Index	Equation	Author
NDVI	$\frac{(NIR - RED)}{(NIR + RED)}$	Rouse, Haas, Deering, Schell, and Harlan (1974)
GNDVI	$\frac{(NIR - GREEN)}{(NIR + GREEN)}$	Gitelson and Merzlyak (1998)
NDRE	$\frac{(NIR - RED\ EDGE)}{(NIR + RED\ EDGE)}$	Maccioni et al. (2001)
MSAVI	$\frac{2*NIR + 1 - \sqrt{(2*NIR + 1)^2 - 8*(NIR - RED)}}{2}$	Qi et al. (1994)

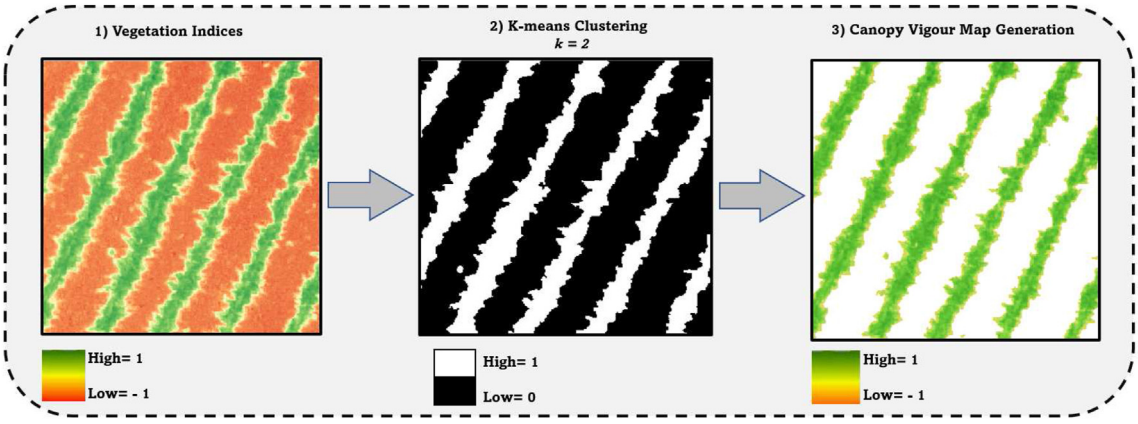

Fig. 4 – Workflow of the unsupervised algorithm proposed for multispectral indices maps by applying K-means clustering. From the first step to the second, soil is identified by the black colour and the remaining set of pixels identifies vines (white colour). In third step the canopy of the vegetation is obtained. (For interpretation of the references to colour in this figure legend, the reader is referred to the Web version of this article.)

consisted of 6 vines and, consequently a total of 84 vines were monitored in VP1. The Total Leaf Area per vine (TLA) was measured using the LI-3100C area meter (Li-COR Biosciences, Lincoln, NE, USA). At harvest, the yield per vine was measured and the number of bunches was counted on each vine per block. The weight of each bunch per vine was determined with a balance (Wunder, mod.60, Milan, Italy). The grape of each vine was crushed, and 100 ml of must were taken to determine the total soluble solid (TSS) (°babo) using a digital refractometer (HANNA Instruments, mod. HI96811, Italy) and titratable acidity (TA) using a Crison Compact Titrator (Crison Instruments, mod. PH-Matic 23, Barcelona, Spain). During winter, SPW was determined using a dynamometer (Wunder, mod. 60, Milan, Italy) on the 84 vines selected at harvest (VP1). In addition to this group of vines (VP1), another 57 vineyard blocks of 6 vines (342 total vines) were identified forming the Vineyard Plot 2 (VP2), where only SPW was measured to perform an accurate analysis of pruning weight prediction. All the analyses were carried out in triplicates.

The six plants of each vineyard block were identified using the coordinates by the GPS STONEX S70G (STONEX® Srl, Milan, Italy) with real-time kinematic correction (RTK) and sub-centimetre accuracy. Through these points it was possible to develop buffers in shape file format on QGIS, with defined dimensions, length of 6 m and width of 0.80 m (Fig. 5).

2.6. *Statistical analysis*

The characteristics of the vegetation indices (count, mean, minimum, maximum, and standard deviation) from the UAV raster images were extracted using the *Zonal statistical* plugin in QGIS. Statistical data extracted from each vegetation index raster were processed using a shapefile with polygons corresponding to the sampling blocks VP1 and VP2, which included only vegetation pixels. The data obtained from the plant measurements were processed with a variance analysis model (ANOVA). The significance level (α) was set at 99% ($p < 0.01$). The null hypothesis (H_0) in the comparison of the

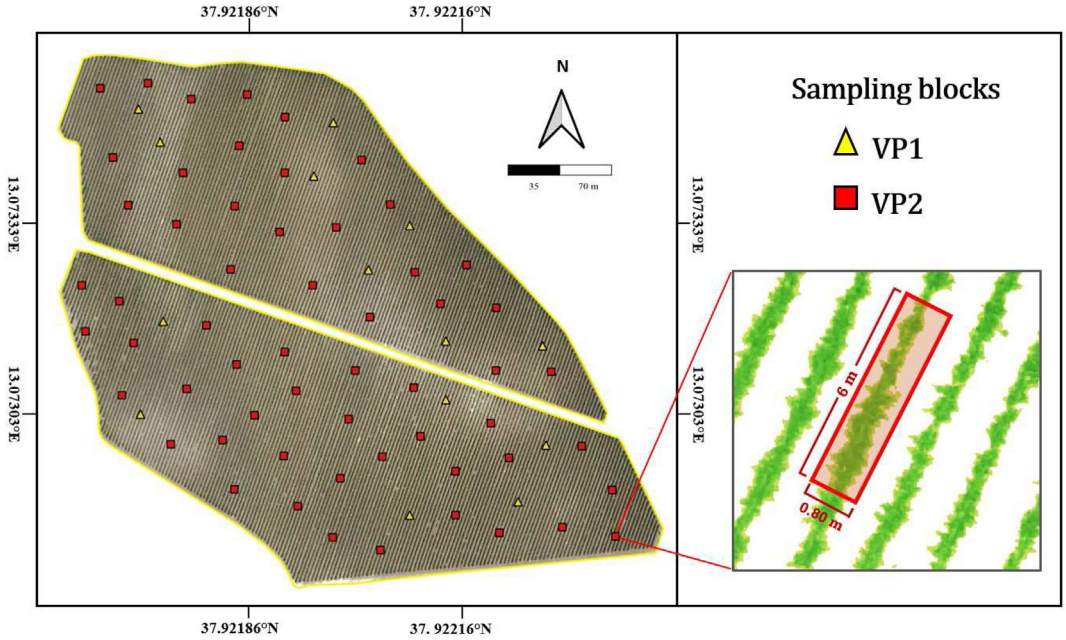

Fig. 5 – Scheme of sampling used in the vineyard plot. Overview of the entire process for identifying the sampling blocks in the field, performed using GCP information to obtain the contours of the sampling polygons.

three groups is that all means are equal, whereas the alternative hypothesis (H_1) is that not all means are equal. Tukey's multiple comparison tests were used to detect the different averages. In addition, the relationships between the vegetation indices and the qualitative parameters of the plants were tested using regression analysis and Pearson's correlation coefficient (r) in the three acquisition times. The difference between slopes was tested using Student's t-test. The SLRM was employed using the multispectral VIs that best correlated with the SPW sampling data. The prediction model was developed based on a SPW training dataset consisting of 3 VP1 sampling blocks and 11 VP2 sampling blocks, equally distributed over the field. Using the SLRM, the SPW prediction of 57 sampling blocks (VP2) was made and then these prediction data were compared with the 57 SPW data observed in the field. Once the model was tested, multispectral VIs data were used for prediction of 1000 SPW values, which were used as input for Kriging to generate the maps. All the statistical procedures were performed using R software (R Core Team, 2020).

2.7. *Geostatistical analysis*

The spatial variability of multispectral indices and the vineyard vigour were conducted using QGIS. Based on a semivariogram and a cross-validation analysis, appropriate models were fitted, and the input parameter employed the ordinary kriging interpolate. This method can express the spatial variation of a specific variable by minimising the distribution error of the predicted values. Kriging interpolation assumes that the estimate at an arbitrary point in a specific zone of the field is expressed with a linear weighting of all observations. To provide the best linear estimation, semivariograms are calculated, which consider the spatial structure (Chiles & Delfiner, 2009; Webster & Oliver, 2007):

$$y(h) = \frac{1}{2N\,(h)} \sum_{i=1}^{N(h)} [Z(xi + h) - Z(xi)]^2 \quad [1]$$

where $N(h)$ represents the number of pairs of observations separated by a value (h), which in turn corresponds to the distance deviation expressed in meters. The parameter $Z(xi)$ is the value of the variable Z at the sampled location xi. The semivariogram, therefore, allows modelling functions to be developed for many infinitely large environmental variables. Therefore, the selection of a semivariogram is critical for geostatistics analysis techniques, as it allows the parameters needed to perform Kriging interpolation to be defined. The selection of the suitable semivariogram was done by calculating the semivariances at different distance intervals (h), fitting specific theoretical models. Isotropic semivariograms were chosen as it was observed that the spatial correlation depends only on the distance module, but not on direction. The experimental semivariogram [1] was adapted through the application of some appropriate theoretical models (Cressie, 2015): the spherical [2] and the exponential ones [3].

$$y(h) = C_0 + C\left[1.5\frac{h}{a} - 0.5\left(\frac{h}{a}\right)^3\right] \quad [2]$$

$$y(h) = C_0 + C\left[1 - exp\left(-\frac{h}{a}\right)\right] \quad [3]$$

In these mathematical models, the input parameters are the sill variance (C_0+C), the range indicated by (a), and nugget variance (C_0), these inputs were calibrated to identify the spatial variability of vineyard vigour. The sill variance

Table 3 – Descriptive statistics of the vegetation indices obtained by UAV multispectral images at different growth stages. The mean value of each index is obtained from 71 replicates ± standard deviation (SD).

	F1	F2	F3
	mean ± SD range	mean ± SD range	mean ± SD range
NDVI	0.64 ± 0.03 0.60–0.68	0.57 ± 0.06 0.51–0.63	0.35 ± 0.05 0.31 ± 0.40
GNDVI	0.46 ± 0.05 0.43–0.49	0.44 ± 0.03 0.40–0.48	0.42 ± 0.05 0.39 ± 0.46
NDRE	0.62 ± 0.03 0.59–0.66	0.33 ± 0.02 0.20–0.36	0.31 ± 0.01 0.18 ± 0.33
MSAVI	0.75 ± 0.04 0.73–0.76	0.68 ± 0.06 0.63–0.73	0.70 ± 0.08 0.66 ± 0.75

concerns the amount of spatial structural variance in the data set. The range represents the distance in which the semi-variogram lies around a limit value. The nugget defines the variability of a sampling interval or analysis error.

In cross-validation, the values estimated from ordinary kriging were compared with the SPW values observed at the sampling points. To check the accuracy of the calculated predicted values for pruning weight estimation, the coefficient of determination (R^2) [4], the root means square error (RMSE) [5] and mean absolute percentage error (MAPE) [6] index were calculated as follows:

$$R^2 = 1 - \frac{\sum_{i=1}^{n}\{y(xi) - y^*(xi)\}^2}{\sum_{i=1}^{n}\{y(xi) - \bar{y}(xi)\}^2} \quad [4]$$

$$RMSE = \sqrt{\frac{\sum_{i=1}^{n}\{y(xi) - y^*(xi)\}^2}{N}} \quad [5]$$

$$MAPE = \frac{100\%}{N}\sum_{i=1}^{n}\left|\frac{y(xi) - y^*(xi)}{y(xi)}\right| \quad [6]$$

where n is the number of points, $y(xi)$ is the measured value, and $y^*(xi)$ is the predicted value, $\bar{y}(xi)$ is the mean value of the observed data. The best prediction model was obtained when the RMSE and MAPE had the lowest value.

3. Results

3.1. Vegetation index data

Table 3 shows the average values and range of the four vegetation indices, showing the minimum and maximum values among the zones considered. These values are distinct for the three flights performed during the growing season and indicated with the letter F, and thus flight F1 was performed at berries pea size stage, flight F2 at beginning of ripening, and F3 at full ripening. The average values of all the indices were lower during the full ripening phase than in the others, except for MSAVI whose lowest values were observed in the veraison phase (F2). The mean values of NDVI and GNDVI, decreased gradually in the three phenological phases. This result can be explained by considering the spectral response of the vegetation in F2, in which the level of photosynthetic activity and efficiency is high, due to the activity of the chlorophyll pigments. Instead, it is difficult to understand the spectral response of NDRE index, again during the F1 monitoring the

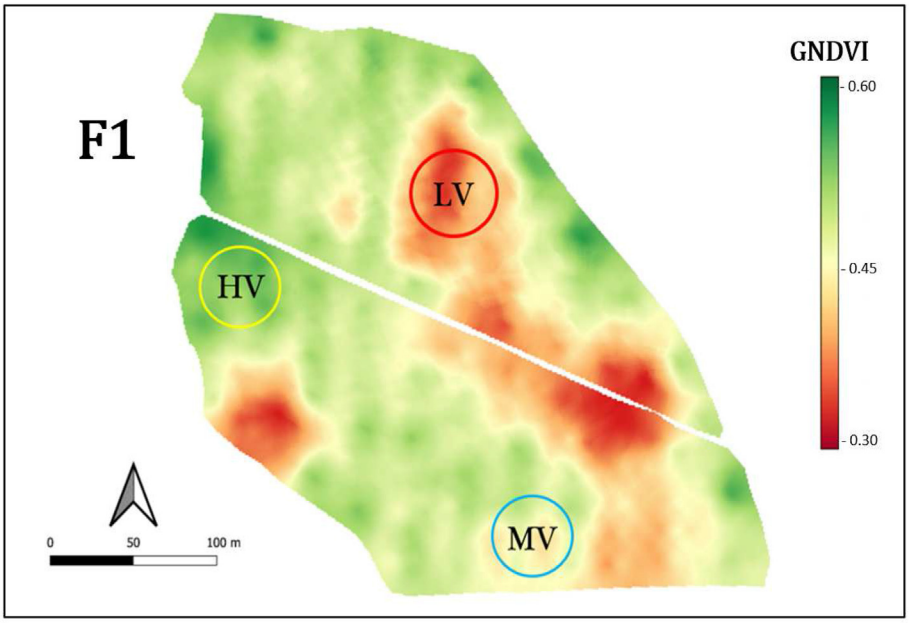

Fig. 6 – Green normalised differential vegetation index map showing the high-vigour (HV), medium-vigour (MV) and low-vigour (LV) vegetation classes derived from a multispectral image remotely sensed by UAV during the F1 survey. (For interpretation of the references to colour in this figure legend, the reader is referred to the Web version of this article.)

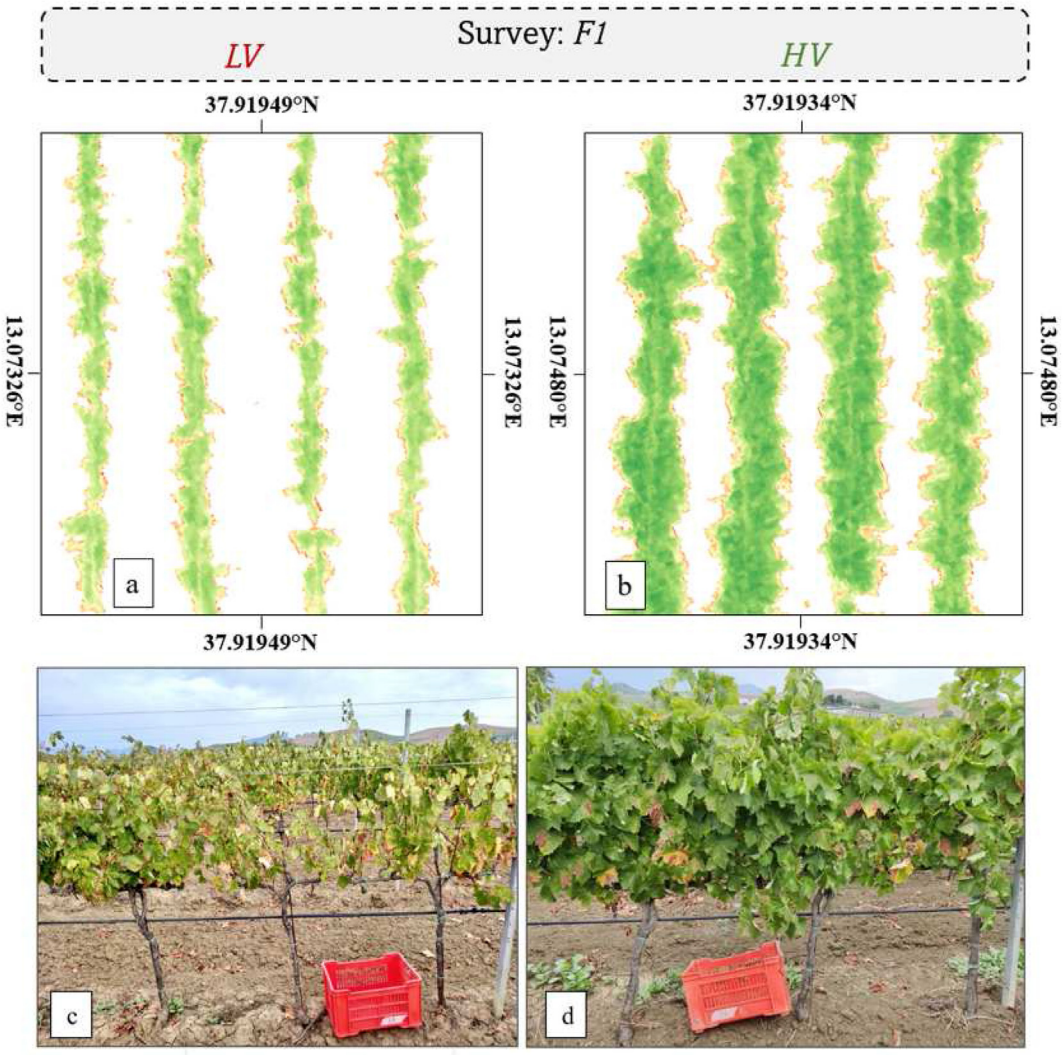

Fig. 7 – GNDVI map with zones of different vigour, (a) section of vineyard row with low vigour (LV), (b) section of vineyard row with high vigour HV). Canopy in LV vines (c), and HV vines (d).

values are within the range 0.59–0.66, as the other indices; in the subsequent phenological phase there is a drastic reduction that continues until the last monitoring.

From the vigour maps generated, different vigour zones were identified by applying the k-means clustering algorithm. For each vegetation index considered, areas of low, medium and high vigour were identified from the first survey F1 (Fig. 6); the determinations made for the subsequent surveys (F2 and F3) confirmed this variability.

Figure 7 (a) and (b) show row sections with different thickness and thus variability in the number of pixels; the differences identified in the rasters were observed in the vineyard, as illustrated in Fig. 7 (c) and (d).

With reference to VP1 blocks, they were distributed in the three vigour levels as follows: 5 blocks in LV zone, 5 blocks in MV zone and 4 blocks in HV zone. The results of the vegetative-productive variability are shown in the boxplots in Fig. 8. With reference to VP2 blocks sampled at pruning, they were distributed in the three vigour levels as follows: 20 blocks in the LV zone, 21 blocks in the MV zone and 16 blocks in the HV zone.

In agreement with the above, it was revealed that there were different growth trends among the vines (VP1) of the three vigour levels identified. The leaf area per vine was higher in HV and MV (3.24 and 2.90 m^2/vine respectively) than in LV vines (2.45 m^2/vine) (Fig. 8 a). Figure 8 b shows how the three vigour levels identified for VP1 vines through the clustering algorithm correspond to three levels of agronomic vigour identified in the field. Indeed, the vines in the LV zones have an SPW average value of 0.29 kg, which is different from high vigour vines (0.47 kg); MV vines, on the other hand, show statistically intermediate values (0.38 kg) between low and HV.

3.2. *Yield and must composition variability*

The descriptive statistics of yield and must quality data are reported in Fig. 9, which shows a wide variability over the different zones detected through the analysis of the UAV images. The vines monitored at harvest (VP1) reported a different number of bunches between low and medium–high vigour vines, as shown in Fig. 9 a The group of vines corresponding to the low vigour (LV) zones had an average of 10

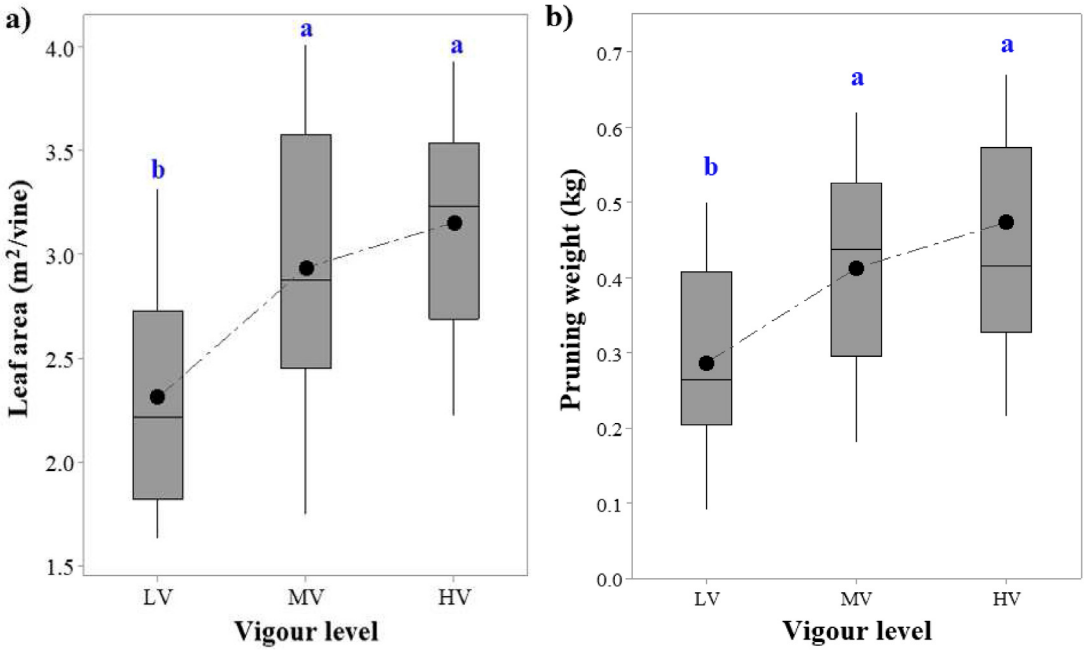

Fig. 8 – Box plots showing the vegetative parameters of the VP1 vines group. (a) Leaf area (b) Shoot Pruning Weight. ● Mean values; data were processed according to Tukey's test with 99% confidence level. Box plot marked with different letters are significantly different ($p \leq 0.01$).

bunches per plant, compared to 14 bunches reported by the high vigour plants. The average bunch weight of the medium and high vigour vines was 66% higher than that of the LV vines (Fig. 9 b). Yield per vine was also significantly different among the groups. It was positively correlated with increasing vigour as illustrated in Fig. 9 c, varying from 1.2 kg in LV to 2.8 kg in HV, corresponding to a potential yield of 5 and 11.3 t ha^{-1} respectively. This higher yield per vine is due both to the higher number and the greater weight of the bunches, as observed in the sampled vines.

The grape quality parameters showed different behaviour between the three vigour levels (Fig. 9 d), the vines from the low vigour zones had a higher soluble solids content (18.3°) than the group of higher vigour vines (17.6°). In view of the above, the vines with a higher yield showed a higher total acidity (5.3 g/L), compared to the vines with a lower yield (4.8 g/L) (Fig. 9 e).

3.3. *Correlation analysis between ground measurements and UAV spectral indices*

Table 4 shows the correlations and relative significance between the vegetation indices and the corresponding values of the quantitative and qualitative parameters of VP1 vines. The first parameter considered was the number of bunches per vine The Pearson index was calculated to find a correlation between the vegetation indices as the number of bunches increased or decreased. However, it was not found a clear trend between the two evaluated variables, as shown by the low values in Table 4. Further considering the variability related to the bunch, the correlation between the indices and the measured weight of bunch was evaluated. Excellent results were found in this case, since the first phenological phase F1 and for the other two surveys carried out. High correlation rates were found, especially for the vegetation indices investigating the spectral response in the red band and red edge. GNDVI also showed a good correlation with bunch weight. However, non-significant correlations between the MSAVI vegetation index and the variable considered were found. For the other two phenological periods examined, excellent significant correlations were found with high values of the Pearson correlation coefficients. Regarding the yield per plant, the results obtained through correlations are in line with those of the average bunch weight. NDVI proved to be a very good predictor of average production per plant. It showed high correlation values of 0.786 in the period in which the first flight was carried out, showing very positive correlations for the two subsequent phenological periods, 0.754 at veraison; the highest correlation of this parameter was found at full berry ripening, equal to 0.806. GNDVI can also be considered a good predictor, but in the phenological periods before ripening it shows a lower correlation than NDVI; when ripening is reached, GNDVI shows a very good correlation with plant yield, equal to 0.839. NDRE was a good predictor in the early phases of crop development with a Pearson correlation index from 0.728 to 0.748 for the phenological phases of berry development and veraison, respectively. After these phases, NDRE showed a lower value and significance than the vegetation indices previously examined. Regarding the only soil-adjusted index, MSAVI, it is not a reliable predictor of production per plant when evaluated at early phenological stages; however, the index proved to be a good predictor of grape yield at veraison with a correlation index of 0.765.

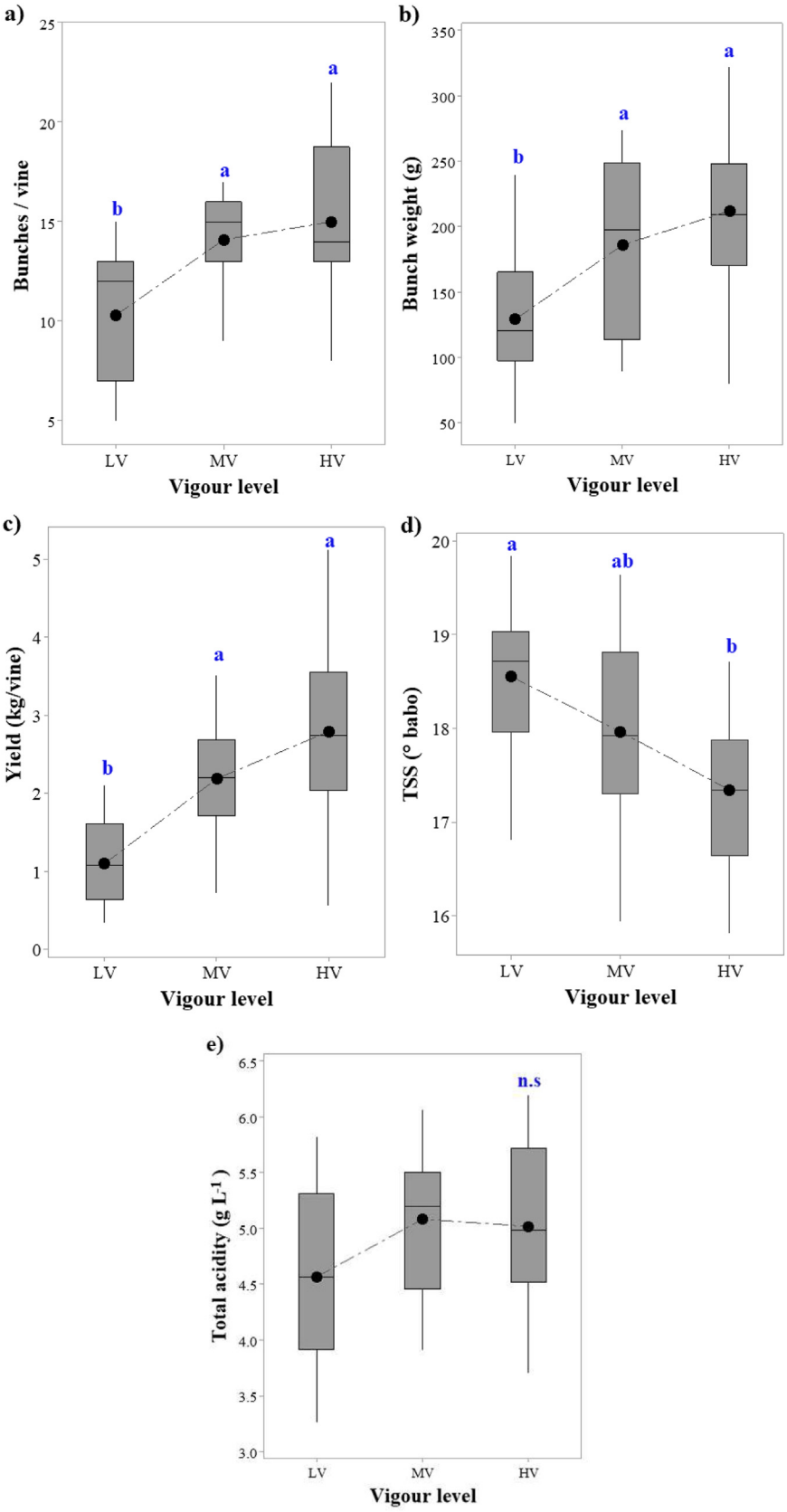

Fig. 9 – Box plots showing the reproductive parameters measured at harvest of the VP1 vines group. ●Mean values; data were processed according to Tukey's test with 99% confidence level. Columns marked with different letters are significantly different ($p \leq 0.01$), n.s = not significant.

Table 4 – Pearson correlation coefficients between agronomic yield variables measured for the VP1 vines group and vegetation indices, with significance *p ≤ 0.05, **p ≤ 0.01, ***p ≤ 0.001, n.s = not significant.

	F1	F2	F3
Bunch/vine			
Spectral indices			
NDVI	0.542*	0.528*	0.314$^{n.s}$
GNDVI	0.307$^{n.s}$	0.382$^{n.s}$	0.444$^{n.s}$
NDRE	0.403$^{n.s}$	0.416$^{n.s}$	0.265$^{n.s}$
MSAVI	0.374$^{n.s}$	0.545*	0.419$^{n.s}$
Bunch weight [g]			
NDVI	0.805***	0.744**	0.770***
GNDVI	0.646**	0.753***	0.875***
NDRE	0.757***	0.767***	0.701**
MSAVI	0.466$^{n.s}$	0.730**	0.739**
Yield [kg per vine]			
NDVI	0.786***	0.754***	0.806***
GNDVI	0.609*	0.687**	0.839***
NDRE	0.728**	0.748***	0.616*
MSAVI	0.504$^{n.s}$	0.765***	0.654**

Table 5 – Pearson correlation coefficients between pruning weight measured for the VP1 vines group and the vegetation indices considered, with significance *p ≤ 0.05, **p ≤ 0.01, ***p ≤ 0.001, n.s = not significant.

Shoot Pruning weight [kg per vine]			
	F1	F2	F3
NDVI	0.844***	0.771***	0.521$^{n.s}$
GNDVI	0.663**	0.696**	0.584*
NDRE	0.759***	0.597*	0.564$^{n.s}$
MSAVI	0.473$^{n.s}$	0.776***	0.655*

Table 6 – Pearson correlation coefficients between grape quality parameters measured for the VP1 vines group and vegetation indices, with significance *p ≤ 0.05, **p ≤ 0.01, ***p ≤ 0.001, n.s = not significant.

Total soluble solids [°babo]			
	F1	*F2*	*F3*
NDVI	- 0.513 **	- 0.391 *	- 0.341*
GNDVI	- 0.760 ***	- 0.722***	- 0.662**
NDRE	- 0.411 **	- 0.651**	- 0.714**
MSAVI	- 0.186$^{n.s}$	- 0.219*	- 0.573**
Total acidity [g L^{-1}]			
NDVI	0.428$^{n.s}$	0.214$^{n.s}$	0.326$^{n.s}$
GNDVI	0.490 *	0.479$^{n.s}$	0.338$^{n.s}$
NDRE	0.462$^{n.s}$	0.466$^{n.s}$	0.426 *
MSAVI	0.063$^{n.s}$	0.306$^{n.s}$	0.539 *

The vegetation indices considered in this study are well correlated with the agronomic variables of grape production. It is relatively easy to identify a phenological period that proves most suitable for evaluating the yield in the vineyard. The highest correlation values were observed at veraison, both in terms of average bunch weight and yield per vine.

In this study, in addition to the evaluation of yield and quality parameters, an important vegetative parameter closely linked to plant vigour was evaluated for VP1 vines, the shoot pruning weight describing the overall growth of the vine. Table 5 shows the correlation data between vegetation indices and SPW. NDVI proves to be a good index in predicting the weight of the pruning mass when evaluated in the phenological phases before veraison. Similar results can be observed for the indices investigated in the green and red edge band, with the only exception of MSAVI which shows a low correlation at the phenological stage of berry growth. On the contrary, MSAVI showed a very positive correlation with SPW at survey F2, also NDVI correlated highly at this phenological stage corresponding to veraison. These results indicate that sampling flights must be carried out during the first periods of vine development to have a more accurate estimation of the pruning mass weight. As berries approach ripeness and senescence processes of the chlorophyll, tissues are triggered, there is a risk of not making a real estimation of this agronomic parameter.

Grape quality parameters correlations with the vegetation indexes are shown in Table 6. Negative Pearson correlation coefficients were found for total soluble solids, indicating that an increase in one of the two variables leads to a reduction in the other and vice versa. This study showed that TSS is well correlated with NDRE with a high statistical significance in the last two surveys. GNDVI also showed a good correlation with this parameter, while NDVI did not show a satisfactory correlation with TSS during the three surveys; in the two phenological stages after the first survey, the statistical significance of the correlation decreased ($p < 0.05$). In addition, the adjusted soil index did not show a good correlation with the previously mentioned quality parameter. In F1 survey, there is no correlation; in the F2 survey, the significance is low ($p < 0.05$); however, the survey in the F3 is an exception, showing a fair correlation ($p < 0.01$). No clear correlations were found about total acidity. In all the phenological periods considered, the correlation indices are not significant except for NDRE and MSAVI indices, which show statistically significant correlation in correspondence with the last sampling flight F3. Based on the results obtained, it can be stated that total acidity could not be easily predicted using multispectral images.

Table 7 – Quantitative relationships between spectral VIs (y) and shoot pruning weight (SPW) (x) of 3 VP1 and 11 VP2 sampling blocks of the vineyard for 2021 growing season.

		Model calibration (VP1 and VP2)		Model validation (VP2)	
Data set	VIs	R^2	Prediction model	RMSE (kg $vine^{-1}$)	MAPE (%)
F1	NDVI	0.81	y = 2.2314 x - 1.0657	0.18	11.21
	NDRE	0.69	y = 2.0928 x - 0.9431	0.24	14.77
F2	NDVI	0.70	y = 1.3475 x – 0.4101	0.30	19.11
	MSAVI	0.67	y = 1.6834 x - 0.7890	0.34	20.51

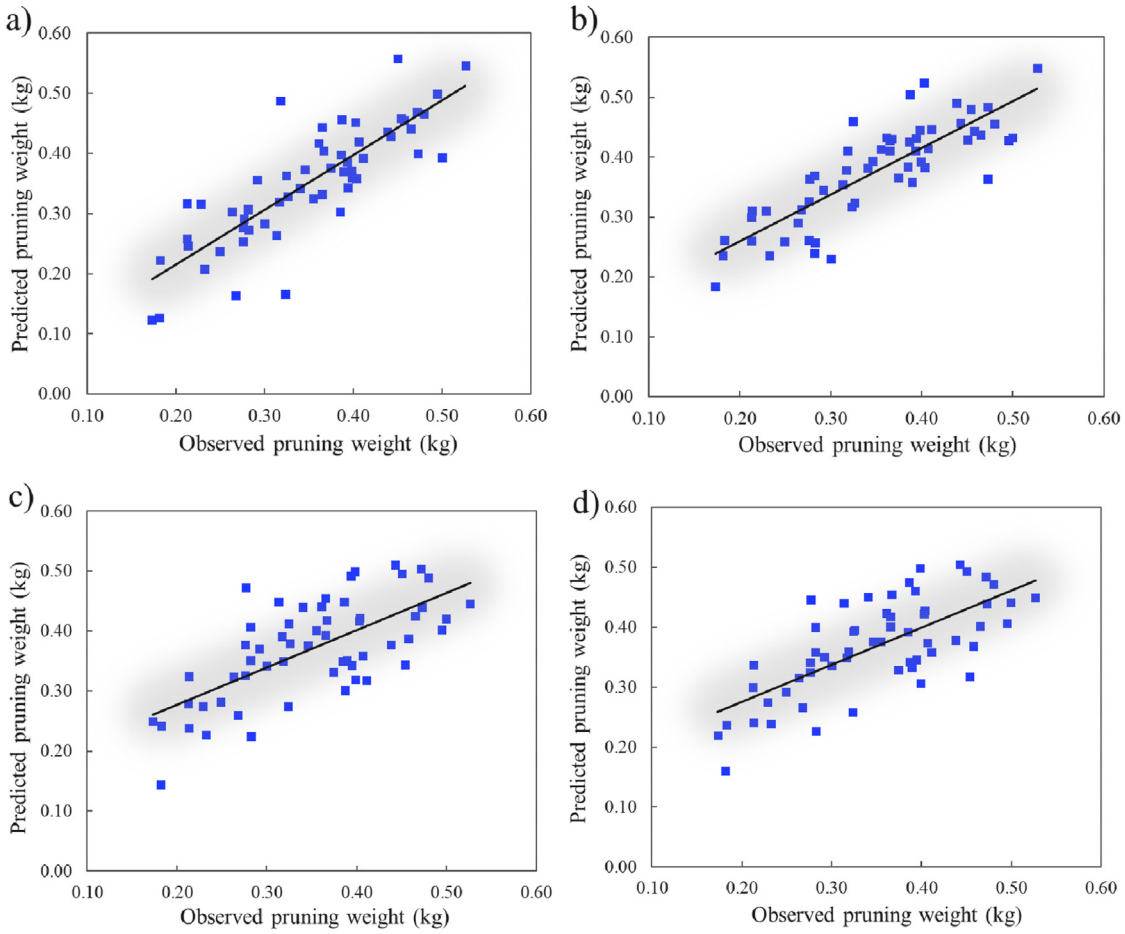

Fig. 10 – Correlation between predicted and observed shoot pruning weight for monitored vines (VP2) using SLRM based on a data set for model validation ($p < 0.001$). (a) correlations developed as a function of NDVI values observed in F1 ($R^2 = 0.69$); (b) NDRE values observed in F1 ($R^2 = 0.69$); (c) MSAVI values observed in F2 ($R^2 = 0.46$); (d) NDVI values observed in F2 ($R^2 = 0.49$).

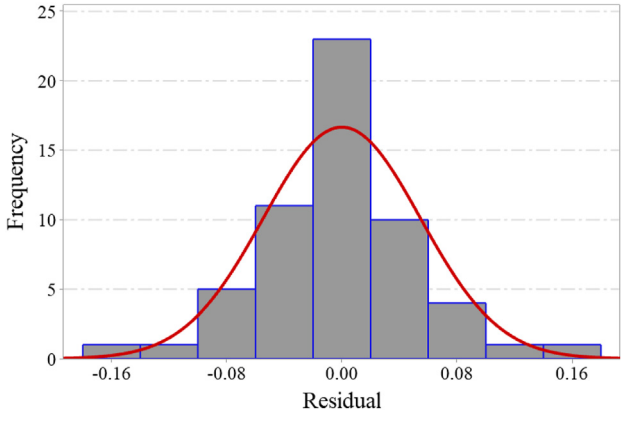

Fig. 11 – Histogram of residual values showing the frequency of each range of values referred to the prediction model using NDVI index data at survey F1.

3.4. *Analysis of prediction model of shoot pruning weight*

After evaluating the correlations among vegetation indices and the key agronomic parameters, it was appropriate to test the validity of the multispectral indices and their possible predictive use. Based on the results of the relationships between SPW and multispectral data, it was decided to continue with the setting up of predictive models with the aim of verifying the validity of these correlations to extend these relationships and information on vegetative growth, to the entire vineyard. Obtaining this information will make it possible to optimise the pruning of the vineyard, adopting a balanced bud load according to the vegetative capacity of the vines. In agreement with the correlation values, NDVI from F1 shows the highest R^2 value, while the other indices, although showing a valid linear regression, remain at lower values (Table 7). The SLRM were developed, which showed a good fit between VIs and SPW, for flight missions F1 and F2. Model

Table 8 – Geostatistical parameters of the fitted semivariogram models for shoot pruning weight predict.

SPW predictive indices	Semivariogram model	Range a (m)	Nugget	Sill variance	Nugget/sill ratio %
SPW NDVI (F1)	Spherical	89	0.001	0.005	20
SPW NDRE (F1)	Exp	110	0.001	0.002	50
SPW MSAVI (F2)	Exp	228	0.001	0.002	50
SPW NDVI (F2)	Exp	233	0.002	0.005	40

Nugget/sill ratio (%) = $[C_0/(c_0+c)]$ x 100.

error metrics were computed, which provide information on the prediction error of the agronomic variable. The best model was based on NDVI index referred to the F1 flight survey, which showed a good linear relationship with pruning weight ($R^2 = 0.81$; RMSE = 0.18; MAPE = 12.8%). The SLRM based on MSAVI, although having a very good correlation with pruning weight, was the index with the highest error value ($R^2 = 0.67$; RMSE = 0.34; MAPE = 20.51%), demonstrating poor reliability in developing predictive calculations on pruning weight.

The relationships between the forecast pruning weight and the observed value, for the four cases studied, are shown in Fig. 10. In Fig. 10 *(a)* the SLRM between the observed SPW (VP2) and the predicted data using the NDVI at F1 as a predictor variable is presented, with correlation $R^2 = 0.69$. Figure 10 *(b)* again shows the linear distribution between the data observed SPW in vineyard (VP2) and those calculated by the prediction model using NDRE index as a predictor, with $R^2 = 0.69$. The application of the model predicting the parameter SPW as a function of the vegetation indices with reference to the period F2, instead, did not provide acceptable results, which can be observed in Fig. 10 *(c)*, *(d)*. Based on the results, it is evident that the prediction correlation of SPW is better in the phenological stages prior to veraison. The prediction of SPW for the 342 vines (VP2) monitored through flight F1 was the most accurate, showing the most stable performance with the lowest RMSE values.

Histograms of the residuals were plotted for all the regression models; Fig. 11 shows only the best regression results identified between the predicted and observed pruning weights calculated from the multispectral NDVI F1 data. The residuals are predominantly concentrated around zero and have a normal distribution, indicating that there are not many outliers.

With the aim of spatialising the prediction data of shoot pruning weight over the entire vineyard area, we applied geostatistics techniques. A semivariogram is used to represent the spatial variation of regionalised variables. Cross-validation is an evaluation technique used to assess the accuracy of results obtained from training data on test data. The estimation accuracy was applied to the data set of values calculated as a function of NDVI, NDRE, and MSAVI referred to F1 and F2. For further clarity on the distribution of variability, the results of some parameters of the geostatistical analyses are reported in Table 8. The semivariogram models that displayed the best fit interpolation for the four datasets considered were the exponential and spherical models. The semivariograms of the predicted pruning weight data calculated based on NDRE (F1), MSAVI (F2), and NDVI (F2) indices were described by the exponential model, reporting a spatial dependence distance of 110(m), 228(m), 233(m) respectively. However, the smallest spatial dependence distance was found by a spherical type semivariogram model, concerning the predicted pruning weight data calculated from NDVI (F1). We calculated the percentage ratio between the fraction of variability not related to distance and the fraction of variability associated with distance; it was found that the lowest values were related to the spherical model.

These statistical analyses highlight the differences among the four data sets, as shown in Fig. 12. The fit of the semivariogram models of the kriging interpolation was based on the values of the cross-validation determination coefficients near the coefficient of the 1:1 line. The value of RMSE refers to the estimation errors in the interpolation of the data and thus in the spatial distribution of the vigour data, this value should be as low as possible. The kriging technique was validated using R-square and RMSE to evaluate the performance and errors associated with the SPW prediction map. The values of R-square were calculated to measure the goodness of fit. The R-square values for the semivariogram models of NDVI and NDRE (Fig. 12 *a* - *b*) calculated based on the F1 surveys, show a good fit, while MSAVI and NDVI indices calculated based on the F2 surveys do not offer an acceptable fit. RMSE values vary from 0.027 to 0.044; these results indicate the accuracy of precision of the prediction models.

Based on the semivariogram concept and models, kriging interpolation methods were evaluated for the spatial distribution of the predicted SPW data in the entire vineyard (Fig. 13). The vegetative vigour showed a heterogeneous distribution in all the four vigour maps, revealing the randomness and dependence of the spatial distribution of vegetative vigour in some areas of the vineyard. Figure 13 *a* shows the spatial distribution of vegetative vigour; this map was developed based on NDVI index data recorded in flight F1. The pruning weight values of the whole vineyard are concentrated around the average values of 0.6 kg. Figure 13 *b* and 13*d*, on the contrary, show SPW values greater than the average weight assessed in the field, and thus the maps tend to provide an overestimation of pruning weight. Figure 13 *c*, referred to the spatial distribution of pruning weight and developed as a function of MSAVI index, on the other hand, shows an underestimation compared to the true value.

4. Discussion

The most significant results obtained in this study are discussed in this section: (i) the analysis of the vineyard spectral response in the three phenological stages; (ii) the correlations between multispectral indices and some vegetative and qualitative characteristics considered; (iii) the analysis of the

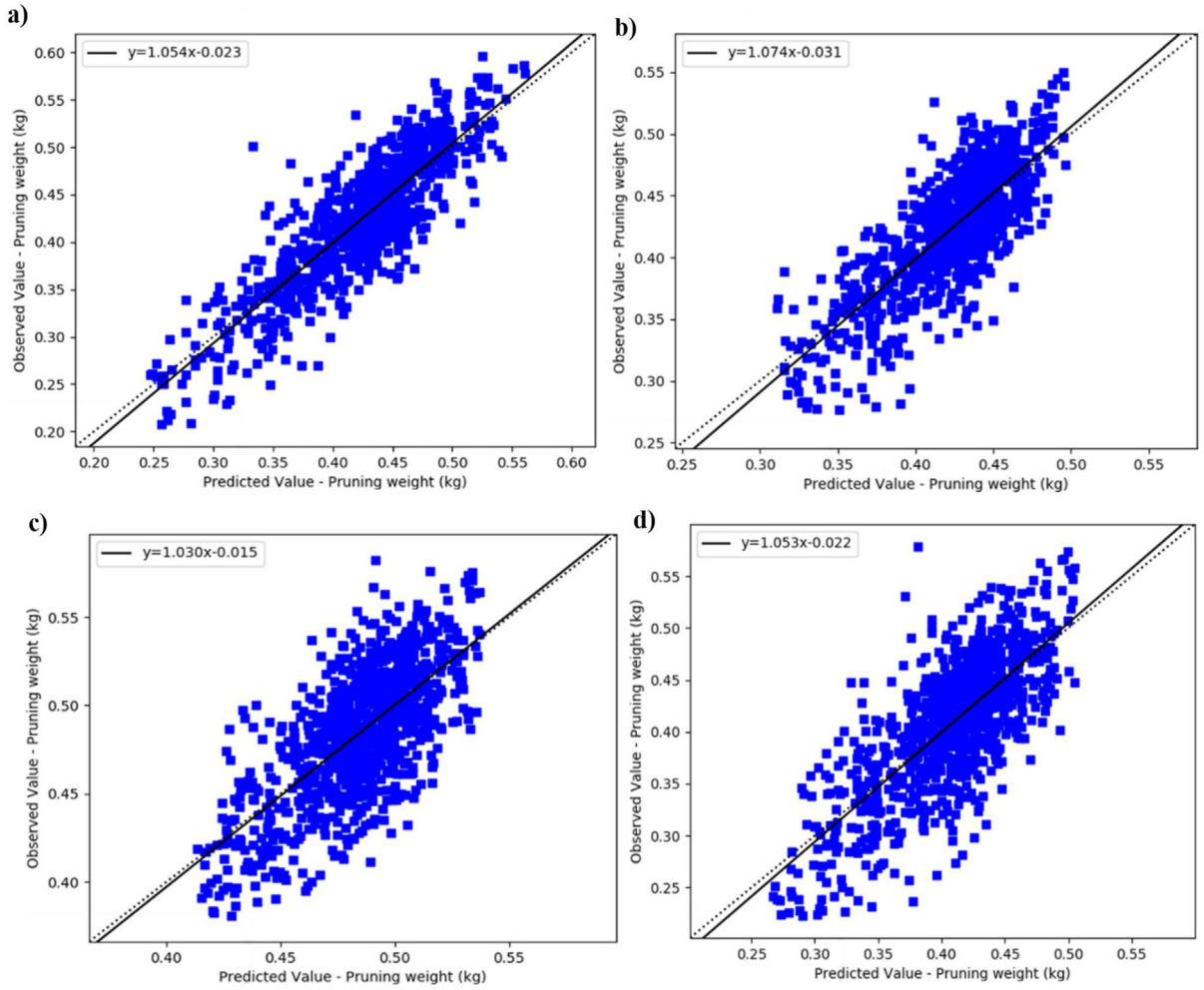

Fig. 12 – Output of cross-validation between the observed and predicted pruning weight data for the regression models developed according to the VIs examined, (a) based on NDVI F1 ($R^2 = 0.75$; RMSE = 0.034); (b) NDRE F1 ($R^2 = 0.61$; RMSE = 0.030); (c) MSAVI F2 ($R^2 = 0.47$; RMSE = 0.027); (d) NDVI F2 ($R^2 = 0.55$; RMSE = 0.044).

prediction shoot pruning weight and then the spatial distribution of vigour according to the indices showing the best correlations with this agronomic parameter.

The data shown in Table 3 concerning the variability of the spectral response of the monitored plots allow an estimation of the level of intra-plot variability. Similarly, the agronomic data presented in Figs. 8 and 9 also show some spatial variability. Pruning weight, which is a very good descriptor of vigour, is one of the parameters that best represents this spatial variability. It shows high variability between low, medium and high vigour plots, in line with other studies (Gatti et al., 2017) conducted in a Mediterranean environment in a non-irrigated vineyard of cv. Barbera cultivated using the trellis system. Also, Matese and Di Gennaro (2021), using UAV-derived multispectral images for surveys on cv. Sangiovese, obtained a distribution in three different vigour levels after performing canopy segmentation of the vineyard. However, three levels of vigour were identified for the multispectral indices considered (Fig. 6), observing the agronomic data; on the other hand, three distinct levels of vigour were not identified, except for the SPW. The temporal dynamics of the four UAV-based multispectral indices studied at the three different phenological stages show average values with a decreasing trend. The highest values were found during the first survey (F1) and then decreased near the last survey, that coincided with the phenological stage of berry ripening. This result can be related to the canopy development; when the first two surveys were performed, the vines were in a phase of intense vegetative growth and therefore the canopies were denser, as obtained by Katsoulas et al. (2016). The last survey was performed at ripeness, when vegetative growth ceased, as a function of which the canopies were sparser (Matese & Di Gennaro, 2021). Also Romboli et al. (2017) identified two vigour levels through UAV surveys in a non-irrigated vineyard in Montalcino (central Italy) of the Sangiovese variety trained on trellis system. NDVI values of the only pixels of the vine canopy of each experimental block were 0.58 ± 0.04 (HV) and 0.36 ± 0.08 (LV). The authors conducted surveys at three

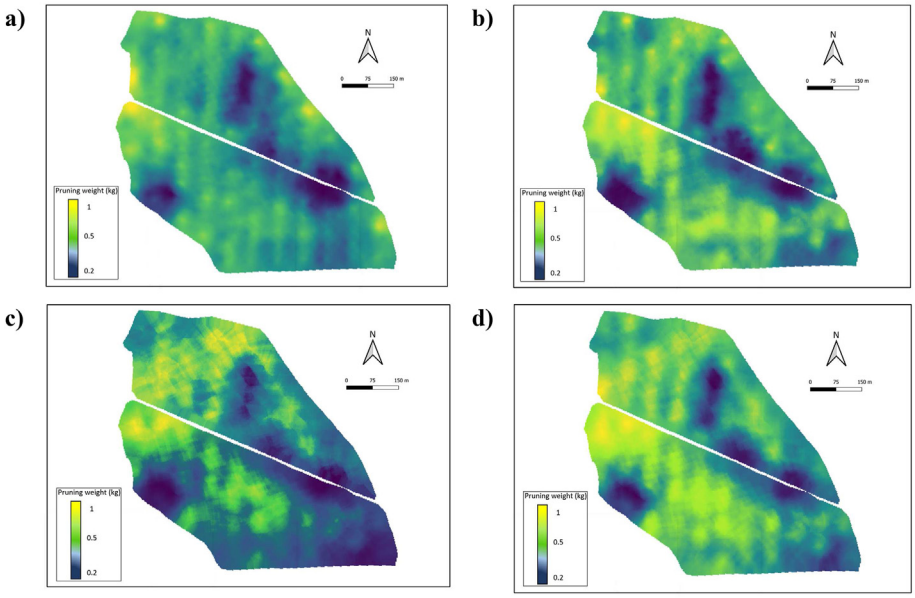

Fig. 13 – Maps obtained by interpolation of predicted pruning weight (kg). Set of points (training): 1000 on all maps. SPW prediction maps calculated as a function of VIs (a) based on NDVI F1; (b) NDRE F1; (c) MSAVI F2; (d) NDVI F2.

phenological periods that coincide with those shown in our study, with NDVI values having a decreasing trend from fruit set phenological stage to ripening for the low vigour level area.

The variability in canopy size development impacts the outcome of the spectral response (Hall, Louis, & Lamb, 2008), as vineyards, not being continuous cropping systems, are affected by the vineyard background (Comba, Gay, Primicerio, & Aimonino, 2015; Rey-Caramés et al., 2015; Turner, Lucieer, & Watson, 2011); by reducing canopy density, the effect of soil background reflectance increases. Some multispectral indices are very sensitive to the effect of soil reflectance, and low LAI values can affect the spectral response (Liu, Pattey, & Jégo, 2012). Furthermore, with the onset of grape ripening, leaf tissues show senescence and chlorophyll pigment degradation phenomena, marked by the progressive yellowing of leaves (Filimon, Rotaru, & Filimon, 2016), which cause a change in canopy reflectance (Pádua, Marques, Hruška, Adão, Peres, et al., 2018). The vine performance in terms of yield, soluble solid content, acidity reported by the vine groups examined shows a different behaviour only between low and high vigour, while the group of medium vigour plants shows agronomic behaviour comparable to the high vigour areas according to the ANOVA. A corresponding vigour distribution was also observed for the agronomic parameter SPW by Gatti et al., 2017, in which the total pruning mass was different in all vigour classes, varying between 0.485 (LV) and 0.895(HV) g/vine. Similar results were also obtained by Bonilla et al. (2013), using multispectral remote sensing images on the Tempranillo variety, in which vigour-related variables such as leaf area and SPW showed significant differences within the three zones. Matese and Di Gennaro (2018) through multispectral UAV surveys carried out during the veraison stage, identified two vigour levels where NDVI data varied between 0.55 (LV) and 0.60 (HV) with corresponding differences in SPW values. In our study, the results for leaf area while not equally distributed across the three vigour levels are significantly different in LV areas compared to HV areas, as Gatti et al. (2017). In their study, LV vines are characterised by less canopy leaf area than HV vines, this may have affected the leaf-to-fruit ratio, a feature noted to influence carbohydrate accumulation in vines (Kliewer & Dokoozlian, 2005).

In our study, TSS shows significant differences between LV and HV zones, the latter showing less accumulation of soluble solids; these results agree with those obtained by Bonilla et al. (2013), Carrillo et al. (2016), Romboli et al. (2017), Gatti et al. (2017).This phenomenon is related to the greater leaf layers in HV vines compared to LV vines; this affects the exposure of the bunch to sunlight and consequently a change in temperature at the berry level, as observed by Dokoozlian and Kliewer (1996). They found that berries grown under lower sunlight conditions from the fruit set stage to ripening have lower soluble solids contents than those of bunches well exposed to sunlight.

No differences in total acidity were found in our study among the three vigour levels; a similar result is reported in Bonilla et al. (2013) and Filippetti et al. (2013).

The relationships between multispectral indices and the quantitative and qualitative parameters of the grape, and vegetative parameters of the vineyard canopy were investigated. Positive correlations were found through Pearson's index computation, especially with bunch weight and yield per vine (Table 4), as well as SPW (Table 5). Pearson's index showed negative correlations with total soluble solids (Table 6); in contrast, no correlation was found with total acidity as well as for the number of clusters. This study shows that high-resolution images captured by UAV can improve the relationships between yield or quality parameters and multispectral indices. For example, very strong correlations with yield data, in all the phenological stages considered, were obtained in contrast to Bonilla et al. (2013), instead (López-

García et al., 2022) found positive correlations between yield and VIs in determined phenological phases, especially considering NDVI, in agreement with the results of this study.

The study of the relationships between technological ripeness and multispectral indices did not provide a clear trend. The relationships between soluble solids and NDVI were not satisfactory, at any of the three phenological stages. Only one multispectral index showed excellent correlation performance with TSS; in effect, GNDVI can be considered in studies predicting the variability of sugar accumulation in grapes. Significant Pearson's correlation values were found for all the relevant phases (Table 6), moreover, a negative correlation between GNDVI and TSS was also found by Maimaitiyiming, Sagan, Sidike, and Kwasniewski (2019) who obtained $r = -0.53$. However, it has been shown that the prediction of soluble solids content of grapes, which is usually performed considering the NIR absorption band, can be influenced by some specific substances such as pigments, carbohydrates and especially the presence of water (Benelli, Cevoli, Ragni, & Fabbri, 2021). The variation in their content depends on ripeness and thus this can influence the result of correlations. The results found in this study are in agreement with other studies conducted by (Anastasiou et al., 2018), in which negative correlations were found through satellite surveys for TSS and NDVI and GNDVI. Among the vegetative variables, pruning weight and its correlations with the spectral indices were mainly considered. The results obtained show that measurements conducted with UAV at pre-veraison phenological stages are more correlated with some multispectral indices than measurements conducted close to grape ripening. The results of the present study confirm the relationship between NDVI and pruning weight found by other authors (Baluja et al., 2012; Dobrowski et al., 2003; Proffitt & Malcolm, 2005; Rey-Caramés et al., 2015). Overall, the obtained multispectral indices showed very good significant correlations with the parameters that are most related to vigour, namely grape yield and shoot pruning weight.

As a result of the correlations observed in this study, we deployed forecast models to monitor the variability of pruning weight and thus vigour of the entire vineyard. The prediction models shown in Table 7 were linear, high coefficients of determination were identified, and low values of RMSE and MAPE were obtained, implying that stable prediction models were selected. Consequently, acceptable coefficients of determination between predicted and observed pruning weights were identified (Fig. 10a and Fig. 10b), with some exceptions for multispectral indices based on the flight of the F2 survey, as shown in Fig. 10c and Fig.10d. To extend these vigour prediction models to the entire vineyard extension (8.2 ha), we performed geostatistical analyses. The four semivariograms obtained provided different information regarding the spatial distribution of vigour. Taking into consideration the pruning weight data obtained with the predictive model based on NDVI (F1), vigour shows a distribution that is closely dependent on the spatial variability of the field and thus not random. In the other cases considered by the prediction models, the semivariogram parameters indicate a weak spatial dependence. Indeed, in agreement with the criteria proposed by Cambardella et al. (1994), in the first case the Nugget variance parameter (C_0) corresponds to a small portion of the Sill variance ($C_0 + C$), and thus the percentage ratio of Nugget/Sill is less than 20% (Table 8). For the second case, the Nugget/Sill ratio is more than 40%, either for the prediction model based on NDRE (F1) or the other two indices MSAVI and NDVI (F2); this typifies the weak spatial dependence. Based on these results, the prediction of SPW and thus vigour that best represents the variability of the vineyard is obtained by taking into consideration NDVI data for the flight performed before veraison. Previous studies confirmed that key vegetative components are a spatially dependent agronomic variable (Baluja et al., 2012; Rey-Caramés et al., 2016); environment predominantly influences the vegetative-productive performance of the vineyard through intrinsic variables such as, for example, the direct effect of soil (Bramley, Ouzman, & Boss, 2011; Tardaguila et al., 2012).

5. Conclusions

This study investigated the capability of a multi-spectral sensor mounted on a multirotor UAV to monitor vegetative indices derived from the spectral response of the vineyard, at different phenological stages of the crop cycle. According to the results obtained by the four multispectral indices studied, it was possible to identify three different vigour levels in the vineyard. Through Pearson's correlation analysis it was found that a large proportion of the agronomic variables showed a stable correlation with the multispectral indices. The correlation analysis between yield components and multispectral surveys performed in the three periods was highly significant. For F1 survey, the indices most correlated with yield were NDVI and NDRE; at veraison and berry maturity, instead, all indices showed a very positive correlation with yield. However, awareness of these correlations at early stages allows corrective operations to be planned and applied throughout the season to improve yield or grape quality. Grape quality parameters were most correlated with multispectral indices investigated mainly in the green band. In fact, GNDVI proved to be the most suitable for representing the variability of grape TSS accumulation, displaying high correlation values starting from the phenological stage of berries pea size. SPW and vegetative vigour should be estimated before veraison, especially using VIs that include the red and near-infrared band. NDVI and NDRE showed high significance of correlation with SPW especially during the phenological stage of berries pea size. At veraison, on the contrary, only NDVI and MSAVI index showed good correlation. Through geostatistical analyses, it was possible to observe that the ordinary kriging method obtained very good interpolation results when using vigour prediction data processed as a function of NDVI from flights performed at preliminary stages of the vineyard crop cycle. These evaluations indicate that among the indices examined, NDVI provides detailed information for the management of crop operations. It was correlated with most of the agronomic parameters considered during the three phenological periods. However, for certain agronomic parameters and in certain phenological stages, the GNDVI and NDRE indices should also be considered.

The UAV sensing system enables the assessment of variability in a mid-range cultivation area, typical of

Mediterranean vineyards, with higher efficiency than manual sensors and more detailed spatial resolution than satellite systems. In addition, we aimed to extend vineyard monitoring techniques with predictive survey methods, thus simplifying the sampling procedure performed in the field and relying on the accuracy of multispectral surveys by obtaining spatial awareness of whole-field variability. Prediction maps can assist farmers in managing subareas of the vineyard with different vigour. SPW prediction maps can guide winegrowers in choosing the appropriate bud load for winter pruning. Finally, these results could be used to develop new pruning management techniques.

Declaration of competing interest

The authors declare that they have no known competing financial interests or personal relationships that could have appeared to influence the work reported in this paper.

Acknowledgments

This work was supported by the project "SiciliAn Micro-nanOTecH Research And Innovation CEnter "SAMOTHRACE" (MUR, PNRR-M4C2, ECS_00000022), spoke 3 - Università degli Studi di Palermo "S2-COMMs - Micro and Nanotechnologies for Smart & Sustainable Communities".

REFERENCES

Aasen, H., Honkavaara, E., Lucieer, A., & Zarco-Tejada, P. J. (2018). Quantitative remote sensing at ultra-high resolution with UAV spectroscopy: A review of sensor technology, measurement procedures, and data correction workflows. *Remote Sensing, 10*(7), 1091.

Anastasiou, E., Balafoutis, A., Darra, N., Psiroukis, V., Biniari, A., Xanthopoulos, G., et al. (2018). Satellite and proximal sensing to estimate the yield and quality of table grapes. *Agriculture, 8*(7), 94.

Assmann, J. J., Kerby, J. T., Cunliffe, A. M., & Myers-Smith, I. H. (2018). Vegetation monitoring using multispectral sensors—best practices and lessons learned from high latitudes. *Journal of Unmanned Vehicle Systems, 7*(1), 54–75.

Baluja, J., Diago, M. P., Balda, P., Zorer, R., Meggio, F., Morales, F., et al. (2012). Assessment of vineyard water status variability by thermal and multispectral imagery using an unmanned aerial vehicle (UAV). *Irrigation Science, 30*(6), 511–522.

Barbagallo, M. G., Guidoni, S., & Hunter, J. (2011). Berry size and qualitative characteristics of Vitis vinifera L. cv. Syrah. *South African Journal for Enology & Viticulture, 32*(1), 129–136.

Barbagallo, M. G., Vesco, G., Di Lorenzo, R., Lo Bianco, R., & Pisciotta, A. (2021). Soil and regulated deficit irrigation affect growth, yield and quality of 'Nero d'Avola'grapes in a semi-arid environment. *Plants, 10*(4), 641.

Barnes, E., Clarke, T., Richards, S., Colaizzi, P., Haberland, J., Kostrzewski, M., et al. (2000). *Coincident detection of crop water stress, nitrogen status and canopy density using ground based multispectral data* (Vol. 1619, p. 6).

Benelli, A., Cevoli, C., Ragni, L., & Fabbri, A. (2021). In-field and non-destructive monitoring of grapes maturity by hyperspectral imaging. *Biosystems Engineering, 207*, 59–67.

Bonilla, I., Toda, F., & Martínez-Casasnovas, J. A. (2013). Grape quality assessment by airborne remote sensing over three years. In *Precision agriculture'13* (pp. 611–615). Springer.

Bramley, R. (2022). Precision Viticulture: Managing vineyard variability for improved quality outcomes. In *Managing wine quality* (pp. 541–586). Elsevier.

Bramley, R., & Hamilton, R. (2004). Understanding variability in winegrape production systems: 1. Within vineyard variation in yield over several vintages. *Australian Journal of Grape and Wine Research, 10*(1), 32–45.

Bramley, R., Ouzman, J., & Boss, P. K. (2011). Variation in vine vigour, grape yield and vineyard soils and topography as indicators of variation in the chemical composition of grapes, wine and wine sensory attributes. *Australian Journal of Grape and Wine Research, 17*(2), 217–229.

Cambardella, C. A., Moorman, T. B., Novak, J., Parkin, T., Karlen, D., Turco, R., et al. (1994). Field-scale variability of soil properties in central Iowa soils. *Soil Science Society of America Journal, 58*(5), 1501–1511.

Campos, J., Gallart, M., Llop, J., Ortega, P., Salcedo, R., & Gil, E. (2020). On-farm evaluation of prescription map-based variable rate application of pesticides in vineyards. *Agronomy, 10*(1), 102.

Candiago, S., Remondino, F., De Giglio, M., Dubbini, M., & Gattelli, M. (2015). Evaluating multispectral images and vegetation indices for precision farming applications from UAV images. *Remote Sensing, 7*(4), 4026–4047.

Caruso, G., Tozzini, L., Rallo, G., Primicerio, J., Moriondo, M., Palai, G., et al. (2017). Estimating biophysical and geometrical parameters of grapevine canopies ('Sangiovese') by an unmanned aerial vehicle (UAV) and VIS-NIR cameras. *Vitis, 56*(2), 63–70.

Catania, P., Comparetti, A., Febo, P., Morello, G., Orlando, S., Roma, E., et al. (2020). Positioning accuracy comparison of GNSS receivers used for mapping and guidance of agricultural machines. *Agronomy, 10*(7), 924.

Catania, P., Orlando, S., Roma, E., & Vallone, M. (2019). *Vineyard design supported by GPS application* (pp. 227–234). https://doi.org/10.17660/ActaHortic.2021.1314.29

Chiles, J.-P., & Delfiner, P. (2009). In *Geostatistics: Modeling spatial uncertainty* (Vol. 497). John Wiley & Sons.

Cinat, P., Di Gennaro, S. F., Berton, A., & Matese, A. (2019). Comparison of unsupervised algorithms for Vineyard Canopy segmentation from UAV multispectral images. *Remote Sensing, 11*(9), 1023.

Comba, L., Gay, P., Primicerio, J., & Aimonino, D. R. (2015). Vineyard detection from unmanned aerial systems images. *Computers and Electronics in Agriculture, 114*, 78–87.

Costa Ferreira, A., Germain, C., Homayouni, S., Da Costa, J., Grenier, G., Marguerit, E., et al. (2007). *Transformation of high resolution aerial images in vine vigour maps at intra-block scale by semi-automatic image processing*.

Cressie, N. (2015). *Statistics for spatial data*. John Wiley & Sons.

Daglio, G., Cesaro, P., Todeschini, V., Lingua, G., Lazzari, M., Berta, G., et al. (2022). Potential field detection of Flavescence dorée and Esca diseases using a ground sensing optical system. *Biosystems Engineering, 215*, 203–214.

del-Moral-Martínez, I., Rosell-Polo, J. R., Uribeetxebarria, A., & Arnó, J. (2020). Spatially variable pesticide application in vineyards: Part I, developing a geostatistical approach. *Biosystems Engineering, 195*, 17–26.

Dobrowski, S., Ustin, S., & Wolpert, J. (2003). Grapevine dormant pruning weight prediction using remotely sensed data. *Australian Journal of Grape and Wine Research, 9*(3), 177–182.
Dokoozlian, N., & Kliewer, W. (1996). Influence of light on grape berry growth and composition varies during fruit development. *Journal of the American Society for Horticultural Science, 121*(5), 869–874.
Droulia, F., & Charalampopoulos, I. (2021). Future climate change impacts on European viticulture: A review on recent scientific advances. *Atmosphere, 12*(4), 495.
Ferrer, M., Echeverría, G., Pereyra, G., Gonzalez-Neves, G., Pan, D., & Mirás-Avalos, J. M. (2020). Mapping vineyard vigor using airborne remote sensing: Relations with yield, berry composition and sanitary status under humid climate conditions. *Precision Agriculture, 21*(1), 178–197.
Filimon, R., Rotaru, L., & Filimon, R. (2016). Quantitative investigation of leaf photosynthetic pigments during annual biological cycle of Vitis vinifera L. table grape cultivars. *South African Journal for Enology & Viticulture, 37*(1), 1–14.
Filippetti, I., Allegro, G., Valentini, G., Pastore, C., Colucci, E., & Intrieri, C. (2013). Influence of vigour on vine performance and berry composition of cv. Sangiovese (Vitis vinifera L.). *OENO One, 47*(1), 21–33.
Galambošová, J., Rataj, V., Prokeinová, R., & Prešinská, J. (2014). Determining the management zones with hierarchic and non-hierarchic clustering methods. *Research in Agricultural Engineering, 60*(Special Issue), S44–S51.
García-Fernández, M., Sanz-Ablanedo, E., Pereira-Obaya, D., & Rodríguez-Pérez, J. R. (2021). Vineyard pruning weight prediction using 3D point clouds generated from UAV imagery and structure from motion photogrammetry. *Agronomy, 11*(12), 2489.
Gatti, M., Garavani, A., Vercesi, A., & Poni, S. (2017). Ground-truthing of remotely sensed within-field variability in a cv. Barbera plot for improving vineyard management. *Australian Journal of Grape and Wine Research, 23*(3), 399–408.
Gatti, M., Squeri, C., Garavani, A., Frioni, T., Dosso, P., Diti, I., et al. (2019). Effects of variable rate nitrogen application on cv. Barbera performance: Yield and grape composition. *American Journal of Enology and Viticulture, 70*(2), 188–200.
Gil, E., Llorens, J., Llop, J., Fàbregas, X., Escolà, A., & Rosell-Polo, J. (2013). Variable rate sprayer. Part 2—Vineyard prototype: Design, implementation, and validation. *Computers and Electronics in Agriculture, 95*, 136–150.
Giovos, R., Tassopoulos, D., Kalivas, D., Lougkos, N., & Priovolou, A. (2021). Remote sensing vegetation indices in viticulture: A critical review. *Agriculture, 11*(5), 457.
Gitelson, A. A., & Merzlyak, M. N. (1998). Remote sensing of chlorophyll concentration in higher plant leaves. *Advances in Space Research, 22*(5), 689–692.
Hall, A., Louis, J., & Lamb, D. W. (2008). Low-resolution remotely sensed images of winegrape vineyards map spatial variability in planimetric canopy area instead of leaf area index. *Australian Journal of Grape and Wine Research, 14*(1), 9–17.
Hunter, J., Volschenk, C., Mania, E., Castro, A. V., Booyse, M., Guidoni, S., et al. (2021). Grapevine row orientation mediated temporal and cumulative microclimatic effects on grape berry temperature and composition. *Agricultural and Forest Meteorology, 310*, Article 108660.
Hunter, J., Volschenk, C., Novello, V., Pisciotta, A., Booyse, M., & Fouché, G. (2014). Integrative effects of vine water relations and grape ripeness level of Vitis vinifera L. cv. Shiraz/Richter 99. II. grape composition and wine quality. *South African Journal for Enology & Viticulture, 35*(2), 359–374.
Jannoura, R., Brinkmann, K., Uteau, D., Bruns, C., & Joergensen, R. G. (2015). Monitoring of crop biomass using true colour aerial photographs taken from a remote controlled hexacopter. *Biosystems Engineering, 129*, 341–351.
Javadi, S. H., Guerrero, A., & Mouazen, A. M. (2022). Clustering and smoothing pipeline for management zone delineation using proximal and remote sensing. *Sensors, 22*(2), 645.
Jorge, J., Vallbé, M., & Soler, J. A. (2019). Detection of irrigation inhomogeneities in an olive grove using the NDRE vegetation index obtained from UAV images. *European Journal of Remote Sensing, 52*(1), 169–177.
Kalisperakis, I., Stentoumis, C., Grammatikopoulos, L., & Karantzalos, K. (2015). Leaf area index estimation in vineyards from UAV hyperspectral data, 2D image mosaics and 3D canopy surface models. *The International Archives of the Photogrammetry, Remote Sensing and Spatial Information Sciences, 40*(1), 299.
Katsoulas, N., Elvanidi, A., Ferentinos, K. P., Kacira, M., Bartzanas, T., & Kittas, C. (2016). Crop reflectance monitoring as a tool for water stress detection in greenhouses: A review. *Biosystems Engineering, 151*, 374–398.
Kemps, B., Leon, L., Best, S., De Baerdemaeker, J., & De Ketelaere, B. (2010). Assessment of the quality parameters in grapes using VIS/NIR spectroscopy. *Biosystems Engineering, 105*(4), 507–513.
Khaliq, A., Comba, L., Biglia, A., Ricauda Aimonino, D., Chiaberge, M., & Gay, P. (2019). Comparison of satellite and UAV-based multispectral imagery for vineyard variability assessment. *Remote Sensing, 11*(4), 436.
Kliewer, W. M., & Dokoozlian, N. K. (2005). Leaf area/crop weight ratios of grapevines: Influence on fruit composition and wine quality. *American Journal of Enology and Viticulture, 56*(2), 170–181.
Liu, J., Pattey, E., & Jégo, G. (2012). Assessment of vegetation indices for regional crop green LAI estimation from Landsat images over multiple growing seasons. *Remote Sensing of Environment, 123*, 347–358.
López-García, P., Ortega, J. F., Pérez-Álvarez, E. P., Moreno, M. A., Ramírez, J. M., Intrigliolo, D. S., et al. (2022). Yield estimations in a vineyard based on high-resolution spatial imagery acquired by a UAV. *Biosystems Engineering, 224*, 227–245. https://doi.org/10.1016/j.biosystemseng.2022.10.015
Lu, J., Cheng, D., Geng, C., Zhang, Z., Xiang, Y., & Hu, T. (2021). Combining plant height, canopy coverage and vegetation index from UAV-based RGB images to estimate leaf nitrogen concentration of summer maize. *Biosystems Engineering, 202*, 42–54.
Maccioni, A., Agati, G., & Mazzinghi, P. (2001). New vegetation indices for remote measurement of chlorophylls based on leaf directional reflectance spectra. *Journal of Photochemistry and Photobiology B: Biology, 61*(1–2), 52–61.
Maimaitiyiming, M., Sagan, V., Sidike, P., & Kwasniewski, M. T. (2019). Dual activation function-based Extreme Learning Machine (ELM) for estimating grapevine berry yield and quality. *Remote Sensing, 11*(7), 740.
Martínez, A., & Gomez-Miguel, V. D. (2017). Vegetation index cartography as a methodology complement to the terroir zoning for its use in precision viticulture. *Oeno One, 51*(3), 289, 289.
Matese, A., & Di Gennaro, S. F. (2018). Practical applications of a multisensor UAV platform based on multispectral, thermal and RGB high resolution images in precision viticulture. *Agriculture, 8*(7), 116.
Matese, A., & Di Gennaro, S. F. (2021). Beyond the traditional NDVI index as a key factor to mainstream the use of UAV in precision viticulture. *Scientific Reports, 11*(1), 1–13.
Matese, A., Toscano, P., Di Gennaro, S. F., Genesio, L., Vaccari, F. P., Primicerio, J., et al. (2015). Intercomparison of UAV, aircraft and satellite remote sensing platforms for precision viticulture. *Remote Sensing, 7*(3), 2971–2990.
Mirás-Avalos, J. M., Fandiño, M., Rey, B. J., Dafonte, J., & Cancela, J. J. (2020). Zoning of a newly-planted vineyard:

Spatial variability of physico-chemical soil properties. *Soil Systems, 4*(4), 62.
Novara, A., Pisciotta, A., Minacapilli, M., Maltese, A., Capodici, F., Cerdà, A., et al. (2018). The impact of soil erosion on soil fertility and vine vigor. A multidisciplinary approach based on field, laboratory and remote sensing approaches. *Science of the Total Environment, 622*, 474–480.
Pádua, L., Marques, P., Hruška, J., Adão, T., Bessa, J., Sousa, A., et al. (2018). Vineyard properties extraction combining UAS-based RGB imagery with elevation data. *International Journal of Remote Sensing, 39*(15–16), 5377–5401.
Pádua, L., Marques, P., Hruška, J., Adão, T., Peres, E., Morais, R., et al. (2018). Multi-temporal vineyard monitoring through UAV-based RGB imagery. *Remote Sensing, 10*(12), 1907.
Pastonchi, L., Di Gennaro, S. F., Toscano, P., & Matese, A. (2020). Comparison between satellite and ground data with UAV-based information to analyse vineyard spatio-temporal variability: This article is published in cooperation with the XIIIth International Terroir Congress November 17-18 2020, Adelaide, Australia. Guest editors: Cassandra Collins and Roberta De Bei. *Oeno One, 54*(4), 919–934.
Pisciotta, A., Barbagallo, M. G., Lorenzo, R. di, & Hunter, J. (2013). Anthocyanin variation in individual'Shiraz'berries as affected by exposure and position on the rachis. *Vitis, 52*(3), 111–115.
Pisciotta, A., Catania, P., Orlando, S., & Vallone, M. (2019). *Influence of row orientation on the canopy temperature of Sicilian vineyards*.
Pisciotta, A., di Lorenzo, R., Barbagallo, M. G., & Hunter, J. (2013). Berry characterisation of cv Shiraz according to position on the rachis. *South African Journal for Enology & Viticulture, 34*(1), 100–107.
Poni, S., Gatti, M., Palliotti, A., Dai, Z., Duchêne, E., Truong, T.-T., et al. (2018). Grapevine quality: A multiple choice issue. *Scientia Horticulturae, 234*, 445–462.
Proffitt, T., & Malcolm, A. (2005). Implementing zonal vineyard management through airborne remote sensing. *The Australian & New Zealand Grapegrower and Winemaker, 502*, 22.
Qi, J., Chehbouni, A., Huete, A. R., Kerr, Y. H., & Sorooshian, S. (1994). A modified soil adjusted vegetation index. *Remote Sensing of Environment, 48*(2), 119–126.
Rey-Caramés, C., Diago, M. P., Martín, M. P., Lobo, A., & Tardaguila, J. (2015). Using RPAS multi-spectral imagery to characterise vigour, leaf development, yield components and berry composition variability within a vineyard. *Remote Sensing, 7*(11), 14458–14481.
Rey-Caramés, C., Tardaguila, J., Sanz-Garcia, A., Chica-Olmo, M., & Diago, M. P. (2016). Quantifying spatio-temporal variation of leaf chlorophyll and nitrogen contents in vineyards. *Biosystems Engineering, 150*, 201–213.
Roma, E., & Catania, P. (2022). Precision oliviculture: Research topics, challenges, and opportunities—a review. *Remote Sensing, 14*(7), 1668.
Román, C., Llorens, J., Uribeetxebarria, A., Sanz, R., Planas, S., & Arnó, J. (2020). Spatially variable pesticide application in vineyards: Part II, field comparison of uniform and map-based variable dose treatments. *Biosystems Engineering, 195*, 42–53.
Romboli, Y., Di Gennaro, S., Mangani, S., Buscioni, G., Matese, A., Genesio, L., et al. (2017). Vine vigour modulates bunch microclimate and affects the composition of grape and wine flavonoids: An unmanned aerial vehicle approach in a Sangiovese vineyard in Tuscany. *Australian Journal of Grape and Wine Research, 23*(3), 368–377.
Rouse, J., Jr., Haas, R. H., Deering, D., Schell, J., & Harlan, J. C. (1974). *Monitoring the vernal advancement and retrogradation (green wave effect) of natural vegetation*.
Sellar, R. G., & Boreman, G. D. (2005). Classification of imaging spectrometers for remote sensing applications. *Optical Engineering, 44*(1), Article 013602.
Siegfried, W., Viret, O., Huber, B., & Wohlhauser, R. (2007). Dosage of plant protection products adapted to leaf area index in viticulture. *Crop Protection, 26*(2), 73–82.
Smart, R., & Robinson, M. (1991). *Sunlight into wine: A handbook for winegrape canopy management*. Winetitles.
Sozzi, M., Bernardi, E., Kayad, A., Marinello, F., Boscaro, D., Cogato, A., et al. (2020). *On-the-go variable rate fertilizer application on vineyard using a proximal spectral sensor*.
Sozzi, M., Kayad, A., Gobbo, S., Cogato, A., Sartori, L., & Marinello, F. (2021). Economic comparison of satellite, plane and UAV-acquired NDVI images for site-specific nitrogen application: Observations from Italy. *Agronomy, 11*(11), 2098.
Sun, L., Gao, F., Anderson, M. C., Kustas, W. P., Alsina, M. M., Sanchez, L., et al. (2017). Daily mapping of 30 m LAI and NDVI for grape yield prediction in California vineyards. *Remote Sensing, 9*(4), 317.
Tardaguila, J., Diago, M., Blasco, J., Millán, B., Cubero, S., García-Navarrete, O., et al. (2012). Automatic estimation of the size and weight of grapevine berries by image analysis. In *2012 International Conference of Agricultural Engineering*.Valencia, Spain: Proc. CIGR-Ageng. July 8-12.
Tassopoulos, D., Kalivas, D., Giovos, R., Lougkos, N., & Priovolou, A. (2021). Sentinel-2 imagery monitoring vine growth related to topography in a protected designation of origin region. *Agriculture, 11*(8), 785.
Taylor, J. A., & Bates, T. R. (2012). Sampling and estimating average pruning weights in Concord grapes. *American Journal of Enology and Viticulture, 63*(4), 559–563.
Tominaga, S., Nishi, S., & Ohtera, R. (2021). Measurement and estimation of spectral sensitivity functions for mobile phone cameras. *Sensors, 21*(15), 4985.
Tosin, R., Martins, R., Pôças, I., & Cunha, M. (2022). Canopy VIS-NIR spectroscopy and self-learning artificial intelligence for a generalised model of predawn leaf water potential in Vitis vinifera. *Biosystems Engineering, 219*, 235–258.
Toth, C., & Jóźków, G. (2016). Remote sensing platforms and sensors: A survey. *ISPRS Journal of Photogrammetry and Remote Sensing, 115*, 22–36.
Triolo, R., Roby, J. P., Pisciotta, A., Di Lorenzo, R., & van Leeuwen, C. (2019). Impact of vine water status on berry mass and berry tissue development of Cabernet franc (Vitis vinifera L.), assessed at berry level. *Journal of the Science of Food and Agriculture, 99*(13), 5711–5719.
Turner, D., Lucieer, A., & Watson, C. (2011). *Development of an Unmanned Aerial Vehicle (UAV) for hyper resolution vineyard mapping based on visible, multispectral, and thermal imagery* (Vol. 4).
Webster, R., & Oliver, M. A. (2007). *Geostatistics for environmental scientists*. John Wiley & Sons.
White, R. E. (2015). *Understanding vineyard soils*. Oxford University Press.
Xue, J., & Su, B. (2017). Significant remote sensing vegetation indices: A review of developments and applications. *Journal of Sensors*. , Article 1353691. https://doi.org/10.1155/2017/1353691, 2017.